Supercell Tornadogenesis over Complex Terrain: The Great Barrington, Massachusetts, Tornado on 29 May 1995

LANCE F. BOSART

Department of Earth and Atmospheric Sciences, University at Albany, State University of New York, Albany, New York

ANTON SEIMON

Earth Institute of Columbia University, Lamont-Doherty Earth Observatory, Palisades, New York

KENNETH D. LAPENTA

National Weather Service Forecast Office, and Center for Environmental Sciences and Technology Management, University at Albany, State University of New York, Albany, New York

MICHAEL J. DICKINSON*

Department of Earth and Atmospheric Sciences, University at Albany, State University of New York, Albany, New York

(Manuscript received 13 December 2005, in final form 6 April 2006)

ABSTRACT

The process of tornadogenesis in complex terrain environments has received relatively little research attention to date. Here, an analysis is presented of a long-lived supercell that became tornadic over complex terrain in association with the Great Barrington, Massachusetts (GBR), F3 tornado of 29 May 1995. The GBR tornado left an almost continuous 50–1000-m-wide damage path that stretched for ~50 km. The apparent rarity of significant tornadogenesis in rough terrain from a supercell well documented in operational Doppler radar motivated this case study. Doppler radar observations showed that the GBR supercell possessed a midlevel mesocyclone well prior to tornadogenesis and that the mesocyclone intensified as it crossed the eastern edge of New York's Catskill Mountains and entered the Hudson Valley. Tornadogenesis occurred as the GBR mesocyclone crossed the Hudson Valley and ascended the highlands to the east. Subsequently, the mesocyclone weakened as it approached the Taconic Range in western Massachusetts before it intensified again as it moved downslope into the Housatonic Valley where it was associated with the GBR tornado. Because of a dearth of significant mesoscale surface and upper-air observations, the conclusions and inferences presented in this paper must be necessarily limited and speculative. What data were available suggested that on a day when the mesoscale environment was supportive of supercell thunderstorm development, according to conventional indicators of wind shear and atmospheric stability, topographic configurations and the associated channeling of ambient low-level flows conspired to create local orographic enhancements to tornadogenesis potential. Numerical experimentation is needed to address these inferences, speculative points, and related issues raised by the GBR case study.

* Current affiliation: Accurate Environmental Forecasting, Inc., Narragansett, Rhode Island.

Corresponding author address: Dr. Lance Bosart, Dept. of Earth and Atmospheric Sciences, University at Albany, State University of New York, 1400 Washington Ave., Albany, NY 12222.
E-mail: bosart@atmos.albany.edu

1. Introduction

Supercell thunderstorms, the convective storm-type associated with most significant tornadoes, occur preferentially over the relatively flat terrain of North America east of the Rockies. In the Rockies and Appalachians of North America, the European Alps, and other midlatitude regions characterized by complex topography, reported tornadoes are much less common. Intriguing questions are whether the fewer reported mountain tornadoes reflect the potential for mountainous terrain to disrupt low-level flows and preclude tornadogenesis in instances that might otherwise yield tornadoes over flat terrain and/or whether significant mountain tornadoes are relatively underreported because fewer people live in the mountains, damage surveys are more difficult to conduct, and fewer structures can be damaged. Although generally not explicitly stated in studies on tornado climatology, anecdotal evidence is that rough terrain is viewed as an inhibitor of tornado occurrence in mountain environments. On occasion, however, large, intense, and long-lived tornadoes have been documented to form from supercells moving over regions characterized by high topographic relief. An event of this type is the focus of this study.

On 29 May 1995, a supercell thunderstorm traveling a corridor across prominent topographic landforms in the northeastern United States produced an almost continuous 50-km-track tornado that caused damage of up to F3 intensity (Grazulis 1997; Fig. 1). The damage swath ranged up to 1 km in width, with severe forest destruction and structural damage reported. Maximum impact was felt in Great Barrington, Massachusetts (GBR), where widespread structural damage occurred and three people were killed when a vehicle was thrown more than 500 m by the tornado (NCDC 1995).

In its size, intensity, longevity, and, most significantly, its occurrence over complex terrain, the GBR tornado represents a rare, but not unique, event. On occasion, tornadic storms form over relatively flat terrain and move into hilly or mountainous regions with their tornadic circulations remaining intact. Examples include the long-track Adirondack tornado in New York State in 1845 (Ludlam 1970); the Shinnston, West Virginia, tornado that killed 103 people during an outbreak on 23 June 1944 (Brotzman 1944; Grazulis 1993); and several tornadoes of the 31 May 1985 outbreak that moved from eastern Ohio into the hilly terrain of northwest Pennsylvania (NCDC 1985; Farrell and Carlson 1989).

Of particular relevance to the present study are other instances when supercells both form and travel across mountainous terrain and produce tornadoes that attain

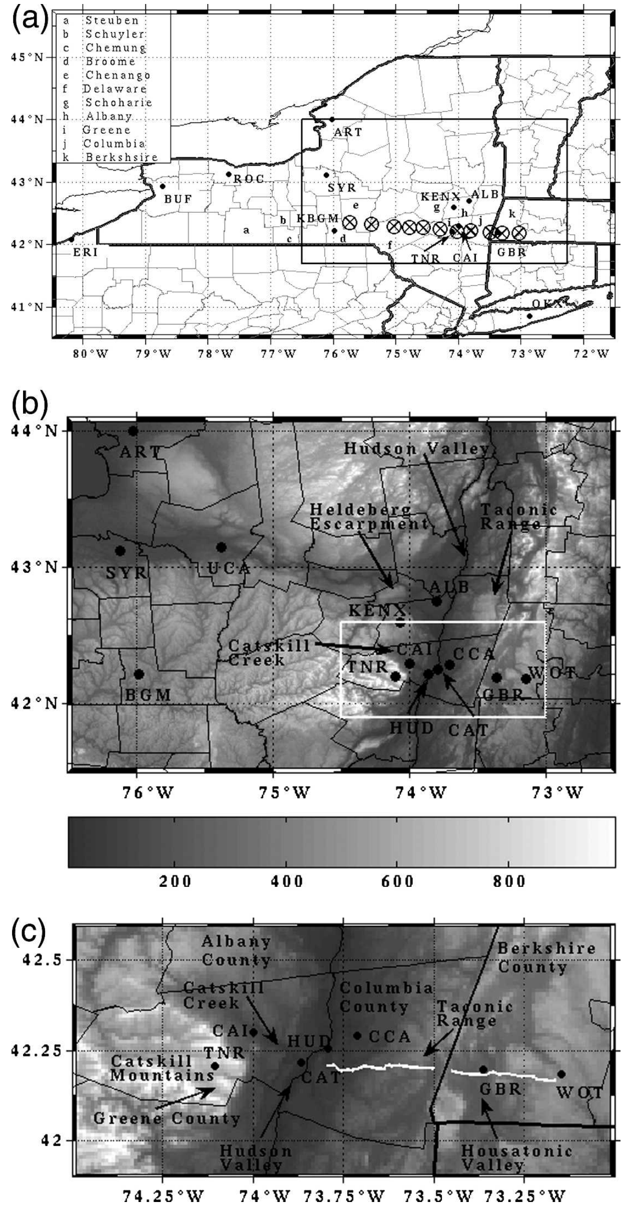

FIG. 1. (a) Station and county identifier map. Counties mentioned in the text are located by lowercase letters and listed in the legend. Encircled crosses denote the track of the GBR supercell from 2002 to 2326 UTC 29 May 1995 at approximately 20-min intervals. The box denotes the domain in (b). (b) Station identifiers and key physiographic features as shown. Terrain height (m) is shaded according to the color bar. The box denotes the domain in (c). (c) Close-up view of principal terrain features, counties, and tornado track (white line). Terrain (m) is shaded as in (b).

strong/violent intensity (F2–F5). Fujita (1989) analyzed an exceptionally large and intense (F4) tornado in forested mountainous terrain in the Teton Wilderness of northwest Wyoming on 21 July 1987. This tornado traveled 39 km, crossed the North American continental divide at an elevation of 3070 m above mean sea level

(MSL), and destroyed an estimated 1 million trees across a damage swath covering 61 km^2. Cases reported elsewhere within the Rockies show that the Teton tornado was not unique for the region. Three significant (≥F2) tornadoes have been documented in the Big Horn Mountains, also in Wyoming (Evans and Johns 1996), including a 13-km-track F3 tornado that destroyed forest at approximately 3000 m MSL on 21 July 1993. A few weeks later another F3 tornado occurred in the Uinta Mountains in northeastern Utah on an intermittent 28-km path that reached a maximum altitude of 3260 m (NCDC 1993). Some lesser-intensity events in the Rocky Mountain region are also noteworthy. To our knowledge, the highest altitude that a tornado has been documented is a ~2-km-track tornado of undetermined intensity that was observed at approximately 3475 m elevation on Longs Peak (4345 m) in the Colorado Rockies on 17 August 1984 (Nuss 1986). A tornado that caused forest damage at 2700 m MSL near Divide, Colorado, on 12 July 1996 was produced by a thunderstorm that displayed relatively conventional supercell structure on a Weather Surveillance Radar-1988 Doppler (WSR-88D), providing confirmation that tornadic supercells are not restricted to low-elevation, low-relief terrain environments (Bluestein 2000).

The GBR tornado occurred over a topographic environment of comparable relief to the Rocky Mountain events listed above, although at lower overall elevations. Terrain in the Appalachian Mountain system of the northeastern United States averages ~2 km lower than the Rockies; however, the magnitude of terrain variations is often comparable in this hilly, forested environment, especially where deeply incised river valleys are located. Despite their rarity, notable tornado events have occurred in the Northeast. In 1878 a tornado struck Wallingford, Connecticut, with 39 resultant fatalities (Ludlam 1970), while the 56-km-track Worcester, Massachusetts, tornado in 1953 caused 94 fatalities; both events have been estimated as F4 intensity by Grazulis (1993). More recently, an F4 tornado along the border of New York and Massachusetts on 28 August 1973 caused six fatalities (NCDC 1973; Grazulis 1993), and an F4 tornado struck Windsor Locks, Connecticut, on 3 October 1979 killing three people and causing $200 million damage (Riley and Bosart 1987). The longest-track tornado (103 km) of the 31 May 1985 outbreak formed and moved across the axis of the Appalachians in Pennsylvania. This tornado attained F4 intensity, had an average width of 1 km [maximum width was ~4 km; Grazulis (1993)] amid densely forested hilly terrain, and destroyed trees at a rate estimated to have reached 1000 trees per second at its widest point (Forbes 1998; G. S. Forbes 2002, personal communication). On 10 July 1989 a large, long-lived supercell crossed the entire breadth of the Appalachians in New York and Connecticut, producing long damage tracks from both tornadoes and severe mesocyclonic winds with widespread devastation and two associated fatalities (Grazulis 1993; Seimon and Fitzjarrald 1994). On 31 May 1998, New York's Hudson Valley witnessed an outbreak of several supercells that produced a series of large, intense tornadoes, including one that reached F3 intensity in hilly terrain at Mechanicville close to the foothills of the Adirondack Mountains (NCDC 1998; LaPenta et al. 2005).

It is noteworthy that all of the cases listed above featured large, long-lived, and intense tornadoes that occurred over hilly terrain amid landforms exhibiting topographic relief ≥150 m at some point along their track. Some characteristics of these selected mountain-area tornadoes recorded in the United States from 1985 to 1998 that formed in complex terrain and went on to produce damage of F3-F4 intensity are compared in Table 1. Elevation differences, rather than absolute elevations, are used to discriminate between what we consider to be mountain versus nonmountain tornado events. This filter is therefore inclusive to Appalachian tornadoes in the eastern United States while it excludes intense tornadoes that occur over the midwestern high plains region, which, although elevated above all but the highest summits of the Appalachians, is characterized by low topographic relief.

The data in Table 1 demonstrate that strong and violent tornadoes in rough terrain environments occur with some regularity, with an event being recorded in the United States roughly once every 2 yr. Their recurrence warrants the attention of the research community because they raise challenging questions concerning how such storms are able to exist in supposedly unfavorable topographic environments. It is plausible that these mountain-area tornadoes might represent an anomalous subset among tornadic storms in aspects other than place of occurrence, and begs the question whether large, intense mountain tornadoes are the product of especially strong supercells overcoming topographic interference (e.g., a supercell with a deep mesocyclone), or whether these tornadoes actually are related to topographic influences upon a supercell.

In contrast to studies on tornadoes in the Midwest, research on tornadoes in California and in central Europe often relates supercell occurrence and tornadogenesis with topographic influences. Orogenic channeling of ambient low-level flows is shown in several case studies to provide both enhanced moisture transport and vertical shear profiles that support supercell development. The recurrence of supercells and tornadoes in

TABLE 1. Selected U.S. mountain-area tornadoes of ≥F3 intensity reported from 1985 to 1998.

Tornado event	Date	Damage F intensity	Length (km)	Width (km)	Topographic variation (m)		Highest damage (m ASL)	Reference
					Tornadic	Supercell		
Moshannon Forest, PA	31 May 1985	F4	103	1.0	530	530	700	Forbes (1998)
Watsontown, PA	31 May 1985	F4	34	0.85	455	455	595	G. S. Forbes (2002, personal communication)
Teton Wilderness, WY	21 Jul 1987	F4	39.2	2.5–4.0*	712	1400	3070	Fujita (1989)
Schoharie, NY	10 Jul 1989	F3	67	1.2	450	1000	650	Seimon and Fitzjarrald (1994)
Litchfield–Hamden, CT	10 Jul 1989	F4	100	1.0–4.0*	650	1200	650	Seimon and Fitzjarrald (1994)
Iraan, TX	1 Jun 1990	F4	35	1.13	220	300	920	NCDC (1990)
Big Horn Mountains, WY	21 Jul 1993	F3	12.9	0.8	600	2000	3020	Evans and Johns (1996)
Uinta Mts, Utah	11 Aug 1993	F3	27.4	0.8	N/A	N/A	3290	NCDC (1993)
Great Barrington, NY–MA	29 May 1995	F3	50	1.0	500	1200	550	Present study
Mechanicville, NY	31 May 1998	F3	48	0.9	150	150	200	LaPenta et al. (2005)

* Damage also attributed to microburst activity and/or intense mesocyclone circulations.
N/A = not available.

association with prominent linear landforms, such as the Po River valley in Italy (Costa et al. 2000), the Rhine Valley in Germany (Hannesen et al. 1998; Hannesen et al. 2000; Dotzek 2001), and the Jura Mountain region in northern Switzerland (Piaget 1976), suggest that such environments may actually enhance the likelihood of supercell and tornado occurrence. Similar findings have been reported in California for the Los Angeles basin (Blier and Batten 1994) and the central and northern San Joaquin Valley (Monteverdi and Quadros 1994), where the channeling of flows by topography creates preferred areas for tornado occurrence. Another notable topography-related tornado frequency anomaly is found near Denver, Colorado, where an orogenic mesoscale circulation, the Denver cyclone, promotes locally favored areas of tornado occurrence (e.g., Szoke et al. 1984). Flow channeling in the north–south-oriented Hudson Valley of New York has been shown to enhance vertical shear profiles that support supercell development (LaPenta et al. 2005).

The synoptic and climatological aspects of significant tornadoes across the Northeast and mid-Atlantic were given by Johns and Dorr (1996) and Giordano and Fritsch (1991). Neither study examined the morphology of individual events (i.e., supercell versus nonsupercell), nor the topographic environments in which these storms occurred. The 1979 Windsor Locks tornado was studied by Riley and Bosart (1987) and its damage patterns were analyzed by Fujita (1993), but highly resolved radar data were lacking for this event, as was the case for the 10 July 1989 supercell that caused sequential tornadoes in New York and Connecticut. The GBR storm was, in contrast, more fortuitous in being observed with Doppler radar (WSR-88D) during both supercell development and the subsequent tornadic phase over complex terrain, thus providing for the opportunity to study tornadogenesis in the context of a supercell's underlying topography. Our analysis, while necessarily limited because of the paucity of surface mesonet observations, will implicate terrain influences in tornadogenesis. It will be suggested that the GBR tornadogenesis was supported by, if not actually attributable to, orogenic modifications of boundary layer storm inflow and outflow as the parent supercell traversed a series of prominent topographic landforms. These key landforms are illustrated in Fig. 2 together with the track of the GBR storm and the tornado damage swaths for reference.

This presentation is organized as follows. The prestorm environment is summarized in section 2 while the mesoscale environment and presupercell stages are described in section 3. Sections 4 and 5 document the developing supercell and pretornadic supercell stages, respectively. A description of the tornadic supercell in the Hudson Valley and the Berkshires appears in section 6 and the concluding discussion follows in section 7.

2. Prestorm environment: 1800 UTC 29 May 1995

The (1963–2002) European Centre for Medium-Range Weather Forecasts 40-yr Re-Analysis (ERA-40)

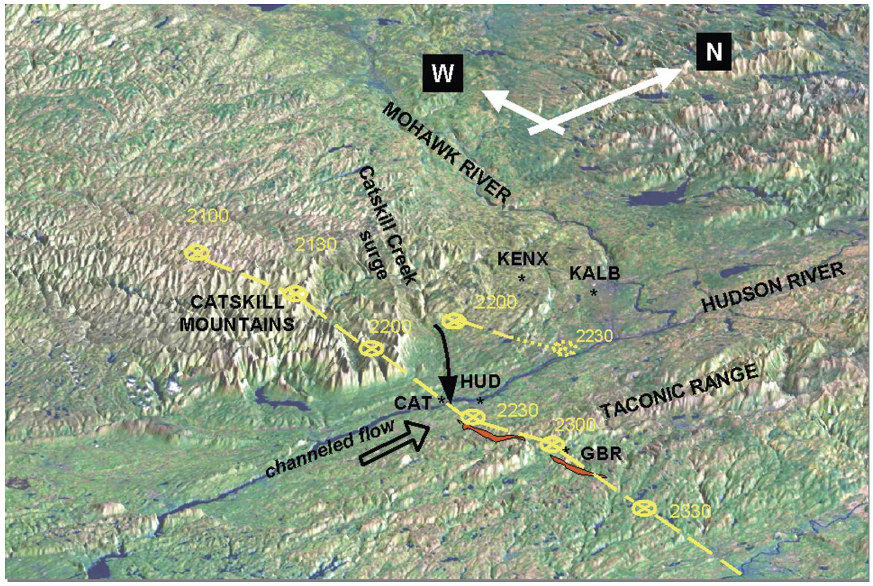

FIG. 2. Simulated oblique aerial perspective looking northwest across the central Hudson Valley region. The long dashed yellow line shows the track of the GBR supercell mesocyclone from 2100 to 2330 UTC 29 May 1995. Encircled yellow x symbols denote mesocyclone positions every 30 min. Shorter yellow line to the north is the track of the left-moving storm (see text) from 2200 to 2230 UTC 29 May 1995. The background image is a cropped section of Landsat imagery draped over a high-resolution (90-m) digital elevation model derived from C-band interferometric radar data from the Shuttle Radar Topography Mission (information online at http://photojournal.jpl.nasa.gov/catalog/PIA02757). The vertical relief is amplified five times.

dataset (information online at http://www.ecmwf.int/products/data/archive/descriptions/e4/) was used to assess the prestorm environment. The ERA-40 gridded datasets, available at a horizontal resolution of 1.125°, were obtained from the National Center for Atmospheric Research. Briefly, by 1800 UTC 29 May a surface boundary had reached central New York and Pennsylvania (Fig. 3a) and storms were forming along and ahead of this boundary near the axis of highest-θ_e air at 850 hPa (Fig. 3b). Winds at 500 and 200 hPa had backed to southwesterly over New York and Pennsylvania ahead of the advancing upper-level trough (Figs. 3a and 3d). The region of storm formation was situated in a 700-hPa ascent region located between the poleward-exit and equatorward-entrance regions of upstream and downstream 200-hPa jets (Figs. 3a, 3c, and 3d). Additionally, the 850–500-hPa temperature difference increased by 4°–6°C over New York and New England between 1200 UTC 29 May and 0000 UTC 30 May, indicative of steeper lapse rates (not shown).

Idealized numerical modeling simulations (e.g., Weisman and Klemp 1982, 1984; Rotunno et al. 1988; Rotunno 1993; Wilhelmson and Wicker 2001) and observational studies (e.g., Johnson and Mapes, 2001; Davies-Jones et al. 2001) of supercells have shown that the environmental vertical shear of the horizontal wind and the convective available potential energy (CAPE) determine the likelihood of supercell formation. The Albany, New York (ALB), and Pittsburgh, Pennsylvania (PIT), 1200 UTC 29 May soundings exhibited surface to 6-km shear values (with veering winds in the boundary layer) of 20–25 m s^{-1}, consistent with reported shear values in tornadic storms in the aforementioned papers (Fig. 4). However, instability was more limited with CAPE and lifted index (LI) values of 0 J kg^{-1} and 7 (246 J kg^{-1} and -1), respectively, at ALB (PIT) (Fig. 4).

The 0000 UTC 30 May ALB sounding was representative of the immediate poststorm environment. Surface to 6-km shear and CAPE values were ~20 m s^{-1} and 414 J kg^{-1}, respectively. At Brookhaven, New York (OKX), located to the south of the main area of convection, the surface to 6-km shear was less (15–20 m s^{-1}) because of a strong southwesterly sea breeze (Fig. 4). The surface-based CAPE value (210 J kg^{-1}) was unrepresentative of the prestorm environment because of the strong sea-breeze-induced cooling in the boundary layer. Lifting the layer of air between 925 and 850 hPa above the inversion yielded a CAPE value of 2000+ J kg^{-1}. This CAPE value was likely more rep-

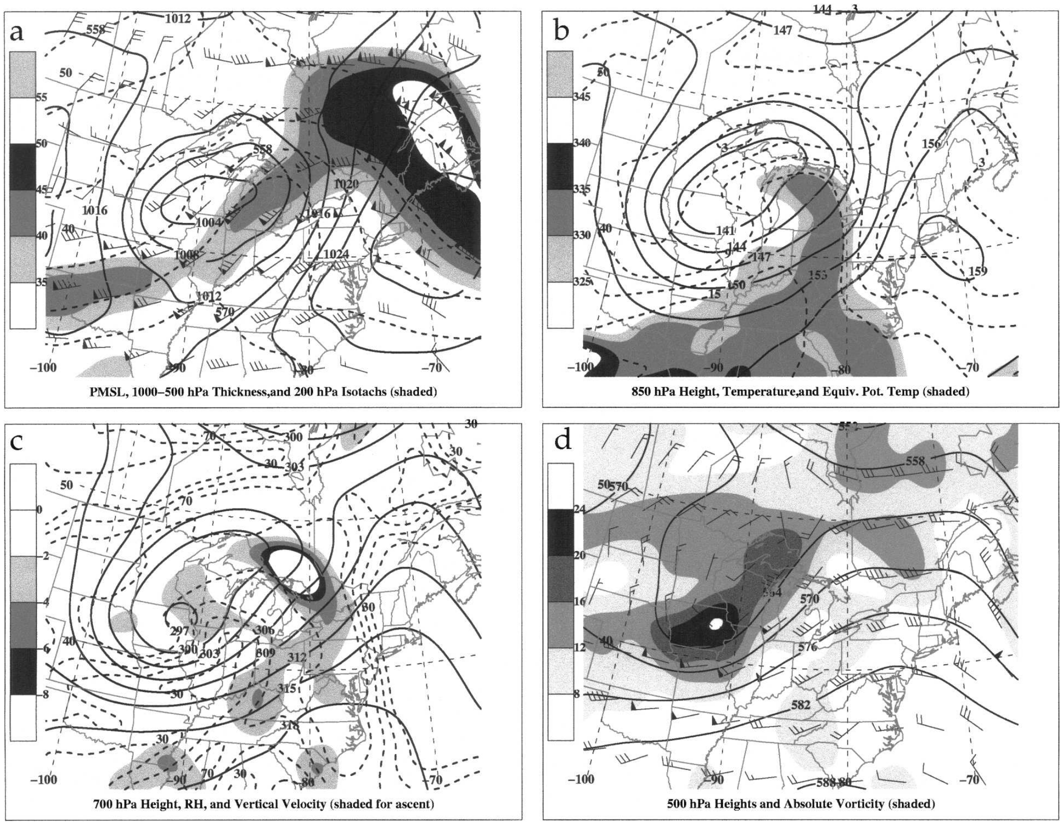

FIG. 3. Synoptic overview for 1800 UTC 29 May 1995: (a) sea level pressure (solid lines every 4 hPa), 1000–500-hPa thickness (dashed lines every 6 dam), and 200-hPa isotachs (shaded beginning at 35 m s^{-1}) according to the scale; (b) 850-hPa heights (solid lines every 3 dam), temperatures (dashed lines every 3°C), and equivalent potential temperature (shaded beginning at 325 K according to the scale); (c) 700-hPa heights (solid lines every 3 dam), percent relative humidity (dashed contours every 20% beginning at 30%), and vertical motion (ascent shaded beginning at -2×10^{-3} hPa s^{-1} according to the scale); and (d) 500-hPa heights (solid lines every 6 dam), winds (m s^{-1}, with pennant, full barb, and half barb denoting 25, 5, and 2.5 m s^{-1}, respectively), and absolute vorticity (shaded beginning at 8×10^{-5} s^{-1} according to the grayscale bar).

resentative of the pre-GBR supercell surface-based environment well inland and together with the observed 0–6-km shear values will support tornadic supercells.

Modified hodographs for the Hudson Valley and the higher terrain to the west based upon the 1200 UTC 29 May ALB sounding (Fig. 4) and the observed midafternoon surface winds showed that terrain-channeled south-southeasterly flow (discussed more fully in section 5b) in the lowest few hundred meters gradually veered to the southwest and west-southwest above 500 m (the hodographs are identical above 1.5 km; Fig. 5). In the higher terrain to the west of the Hudson Valley, where there was no terrain channeling of the low-level southerly flow, the length of the clockwise-turning hodograph was shorter. Based upon a radar-determined GBR tornadic supercell storm motion of 272° at 13 m s^{-1}, storm-relative helicity values of ~325 $m^2 s^{-2}$ (250 $m^2 s^{-2}$) were estimated for the Hudson Valley (higher terrain) hodograph. On the basis of the large-scale environmental structure (Fig. 3) and the sounding analyses (Figs. 4 and 5), the environment was favorable for supercell formation over eastern New York and western New England so the modest outbreak of severe thunderstorms, including several supercells, was unsurprising. According to the 1500 UTC 29 May convective outlook released by the Storm Prediction Center (SPC), SPC forecasters indicated that "wind profiles appear supportive of a few isolated supercells, with tornadoes not out of the question, especially if the low-level flow remains slightly backed in the vicinity of a retreating cool air mass in northern portions of the moderate risk area."

At 1315 UTC 29 May an area of clear skies was evident in the visible satellite imagery from western New York to the western Adirondacks ahead of an area of cumuliform clouds over extreme western New York

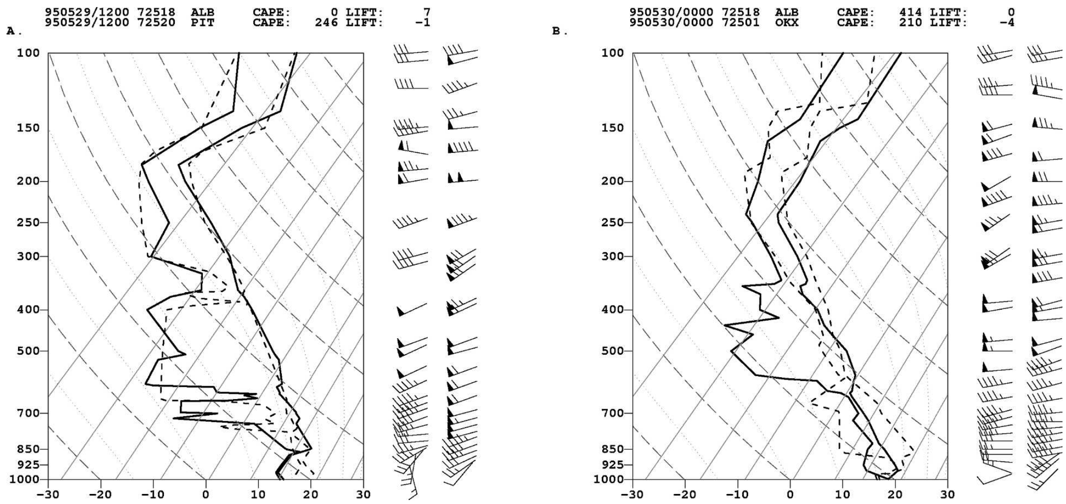

FIG. 4. Observed soundings in skew T–log$p$ format. (left) ALB (solid) and PIT (dashed) at 1200 UTC 29 May 1995 with PIT winds plotted to the right of the ALB winds. (right) Same as in left panel but for ALB (solid) and OKX (dashed) at 0000 UTC 30 May 1995, with the OKX winds plotted to the right of the ALB winds. Full pennant, barb, and half barb denote wind speeds of 25, 5, and 2.5 m s^{-1}, respectively. CAPE (J kg^{-1}) and LI values appear at the top of the sounding panels.

and Pennsylvania (Fig. 6a). By 1615 UTC, lines of cumuliform clouds had formed in the former clear slot over western New York (Fig. 6b), consistent with the developing broken line of storms at 1754 UTC (section 3). By 1915 UTC the broken line of storms had organized and thunderstorms were apparent (section 3). The supercell that was destined to become the tornadic GBR storm was evident behind this leading broken line of storms near 42.5°N and 76.5°W at 1915 UTC (Fig. 6c). By 2215 UTC the GBR supercell had reached the Hudson Valley after moving off the high terrain of the Catskills and was marked by a region of overshooting convective cloud tops near 42.3°N and 73.7°W (Fig. 6d).

3. Mesoscale environment/presupercell stage: 1700–2000 UTC 29 May 1995

a. Surface features

Conventional forcing mechanisms were instrumental in spawning severe convection as shown by a manually analyzed surface map for 1800 UTC 29 May that revealed a prefrontal trough that stretched from north-

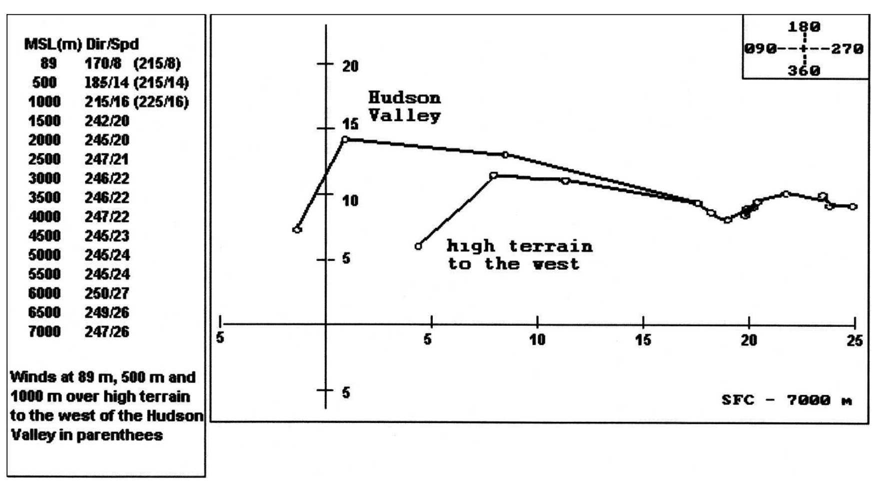

FIG. 5. Representative estimated hodographs for the Hudson Valley and the higher terrain to the west over the Catskills valid at approximately 2000 UTC 29 May 1995, just prior to tornado development. Winds in the lowest 1.5 km were modified based on the observed surface winds in the Hudson Valley and over the higher terrain of the Catskills to the west. Winds above 1.5 km are based on the 1200 UTC 29 May 1995 ALB sounding.

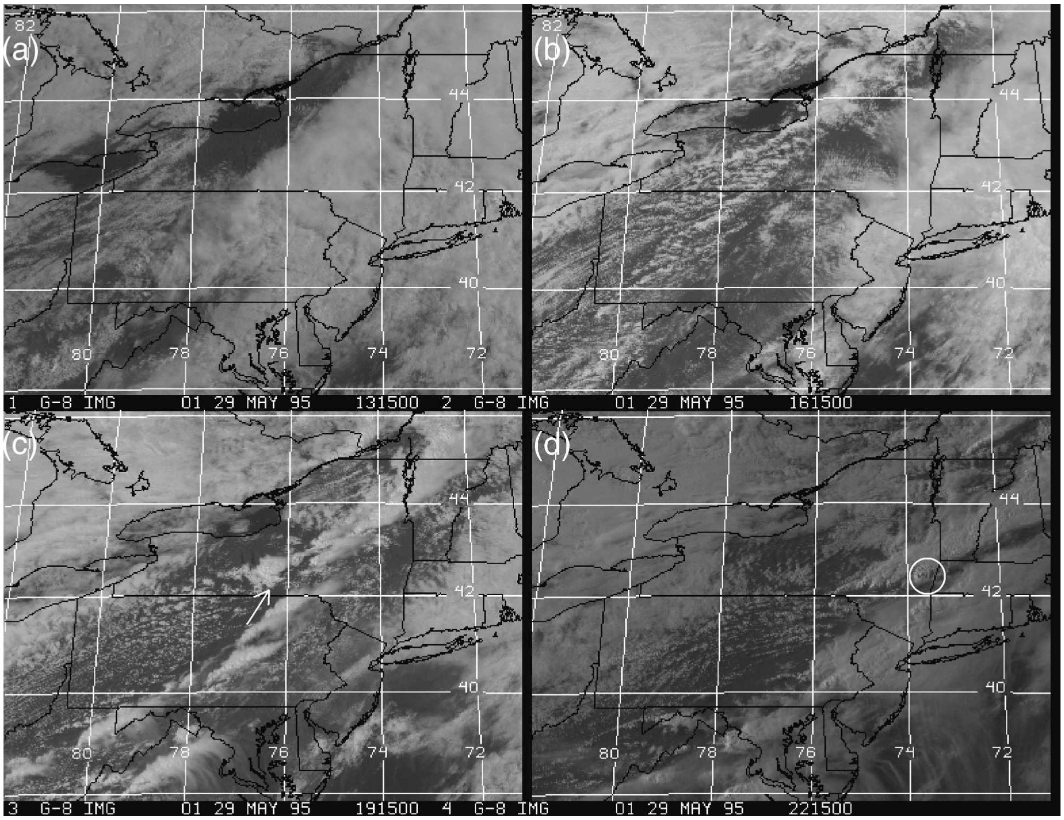

FIG. 6. Visible satellite imagery from the *Geostationary Operational Environmental Satellite-8* at (a) 1315, (b) 1615, (c) 1915, and (d) 2215 UTC 29 May 1995. White arrow in (c) points to the developing GBR storm. White circle in (d) denotes the GBR supercell.

western New York to central Pennsylvania (Fig. 7a). A ribbon of high-θ_e air (>336 K), upon which developing thunderstorms over central New York were feeding, had surged poleward ahead of this trough (Fig. 7b). This high-θ_e air surge occurred ahead of the upper-level trough in a region of 700-hPa ascent between the upstream and downstream 200-hPa jets (Figs. 3 and 6). In central New York at Binghamton (BGM) the arrival of the prefrontal trough resulted in a wind shift from southwest to northwest near 2100 UTC and a more pronounced and likely thunderstorm-driven temperature decrease (approximately 4°–5°C in 3 h; Fig. 8a). In east-central New York at Utica (UCA), north-northeast of BGM, it was difficult to distinguish between the prefrontal trough wind shift and the passage of an outflow boundary associated with a reported thunderstorm near 1900 UTC (not shown). The wind shifted to the northwest and the temperature decreased 4°C with moderate rainshowers near 1900 UTC. The wind at UCA backed briefly to southerly before the prefrontal trough, accompanied by a wind shift back to northwest and a 5°C dewpoint decrease, arrived between 2000 and 2100 UTC.

Meanwhile, the outflow boundary advanced down the Mohawk Valley and near 2200 UTC 29 May reached ALB, where a thunderstorm was reported (Fig. 8b). A comparison of the BGM and ALB meteograms reveals that surface winds ahead of the convection at BGM were from the south-southwest while at ALB the winds were from the south-southeast in response to channeled flow up the Hudson Valley (Figs. 8a and 8b). These surface wind direction differences were very similar to those observed prior to the development of the 31 May 1998 Mechanicville, New York, F3 tornado and likely attest to the importance of terrain-channeled low-level southerly flow in the Hudson Valley in severe storm modulation [discussed more fully in sections 4 and 5; LaPenta et al. (2005)]. This channeling process is illustrated, along with regional landforms, the track of the GBR supercell, and the tornado damage path, in Fig. 2.

b. Radar signatures

At 1702 UTC 29 May an isolated reflectivity core near Bradford, Pennsylvania (BFD), west of a southwest–northeast broken line of showers and thunder-

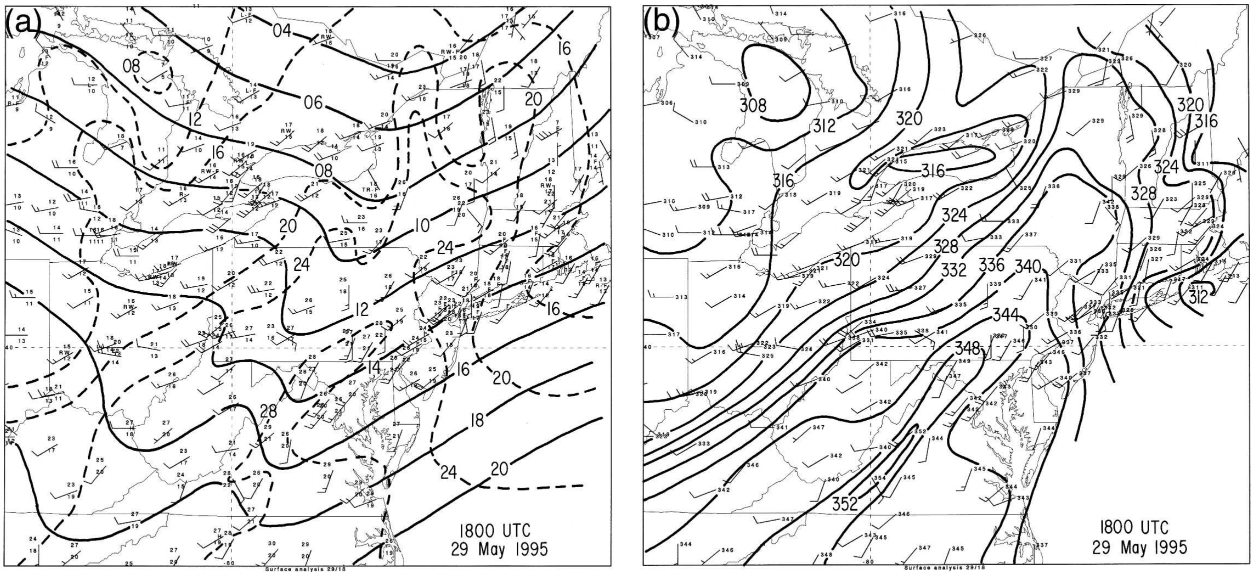

FIG. 7. (a) Surface map at 1800 UTC 29 May 1995. Isobars (solid) every 2 hPa. Isotherms (dashed) every 4°C. Surface observations are plotted conventionally. (b) As in (a) but for equivalent potential temperature (solid) every 4 K.

storms associated with the prefrontal trough, marked the initiation of the storm that subsequently moved eastward and became the GBR tornadic supercell (not shown). By 1754 UTC this reflectivity core had moved east-northeast across the New York border and was located behind a patch of weaker convective cells (Fig. 9a). Radial velocity data from the 0.5° scan of the KBGM radar, located at BGM, indicated that the storm at this time exhibited weak cyclonic rotation as judged by an estimated 5–10 m s^{-1} rotational velocity difference measured over 5–10 km (not shown; KBGM was inoperative from 1823 to 1840 UTC). By 1904 UTC new convection developed over the higher terrain along the southern edge of the storm (Fig. 9b), grew in areal coverage, and spread northward toward the location of the main storm (Fig. 9c). Subsequent to 1954 UTC, the cyclonic circulation became better defined (Fig. 10) and began moving to the right of the mean flow (KENX radar located near Albany, see Fig. 1b for location, first indicated a mesocyclone at 2000 UTC in this storm).

By 2008 UTC 29 May (not shown) the GBR supercell was still the southernmost storm in the broken line of storms. KBGM radial velocity data from the 0.5°–6.0° elevation scans (not shown) all showed a rotational velocity couplet (maximum shear of 20 m s^{-1} across 5 km at an elevation of 2.2 km above ground level) with this storm. By 2057 UTC the supercell reached the western Catskills (northeast of BGM)

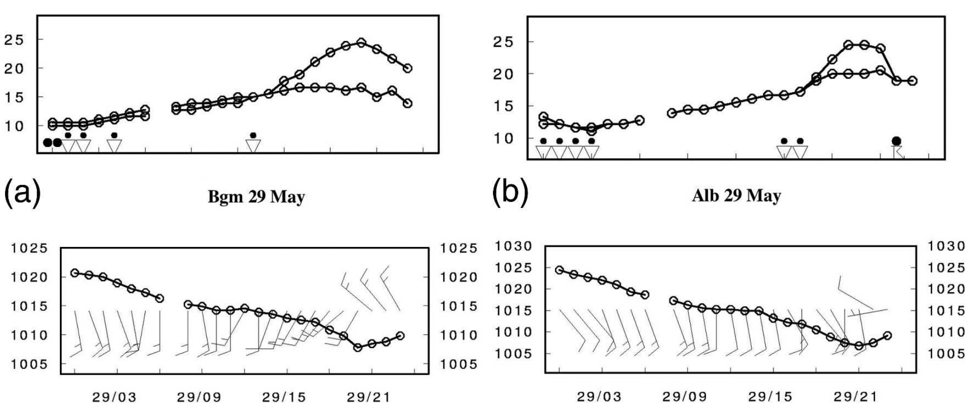

FIG. 8. Meteograms of surface weather for (a) BGM and (b) ALB. (top) Temperature and dewpoint temperature (°C) and reported weather (conventional symbols). (bottom) Station altimeter settings (hPa) and winds (m s^{-1}, as in Fig. 3). Station locations are shown in Fig. 1b.

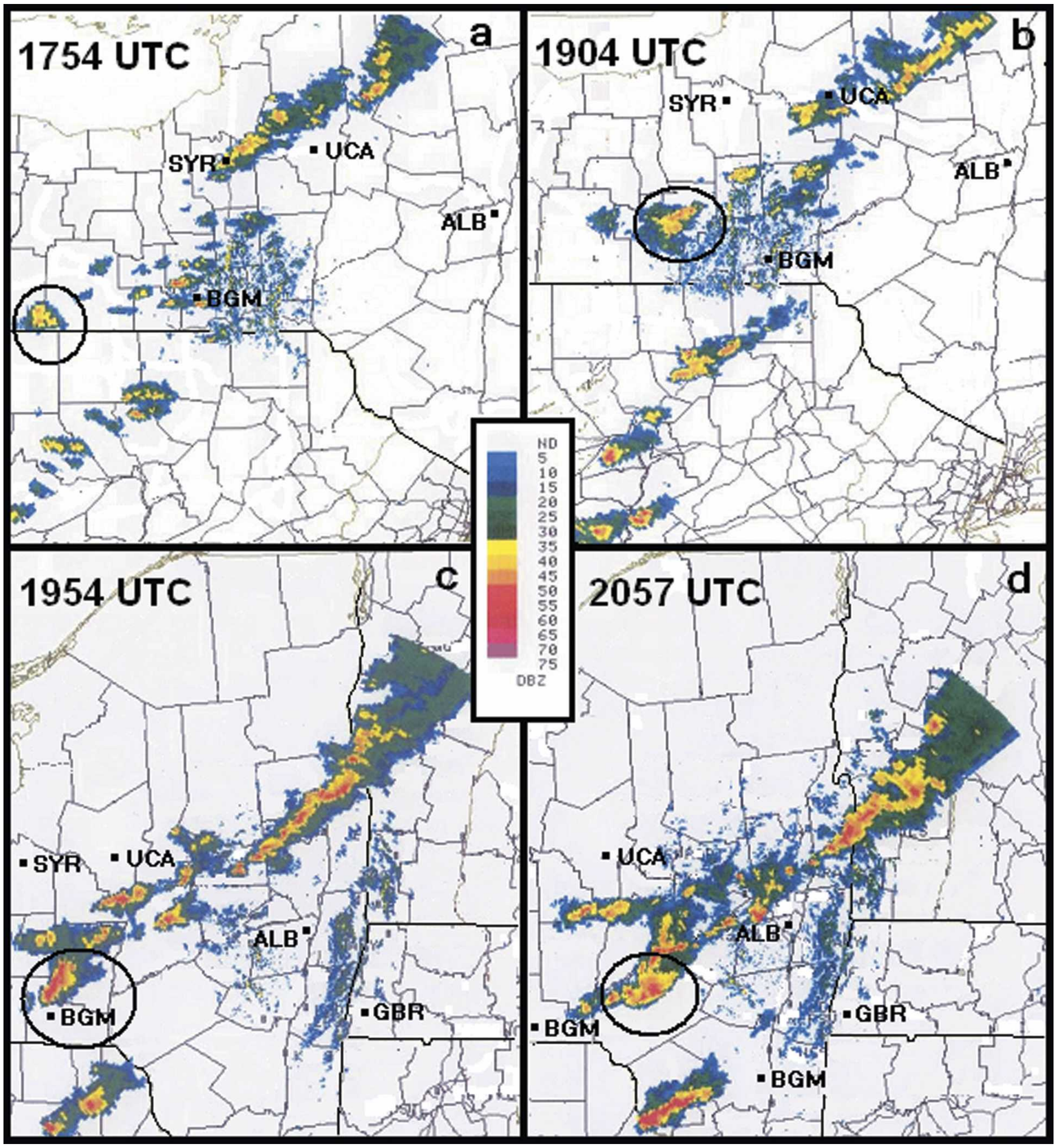

FIG. 9. Radar base reflectivity maps for 29 May 1995 from a 0.5° scan from KBGM at (a) 1754 and (b) 1904 UTC and from KENX at (c) 1954 and (d) 2057 UTC. Units are in dBZ according to the color table. Black ovals indicate the location of the developing GBR storm.

while a second storm developed 10–15 km behind the outflow boundary to the north-northeast of the supercell (Fig. 9d). This second storm was of significance later, during the tornadic phase of the supercell, and is discussed more fully in sections 5a and 5b. Also after 2057 UTC, the supercell compacted as the areal coverage of the 35-dBZ reflectivity contour decreased along the northeastern edge of the storm while relatively high reflectivities were sustained in the storm core.

A time series of radar-derived rotational velocities for selected radar beam elevation levels is used to summarize the presupercell stage of the GBR storm (Fig. 10). The rotational velocity increased from approximately 10 m s^{-1} at 1913 UTC to 15–16 m s^{-1} at 2052 UTC 29 May in the 0.5° and 1.5° scans. A rotational velocity of 15 m s^{-1} was also computed for the 2.4° scan beginning just before 2052 UTC, indicative of a strengthening mesocyclone in the GBR supercell below 700 hPa as it approached the western Catskills (Fig. 10) and in agreement with the radar-indicated storm compaction (Fig. 9).

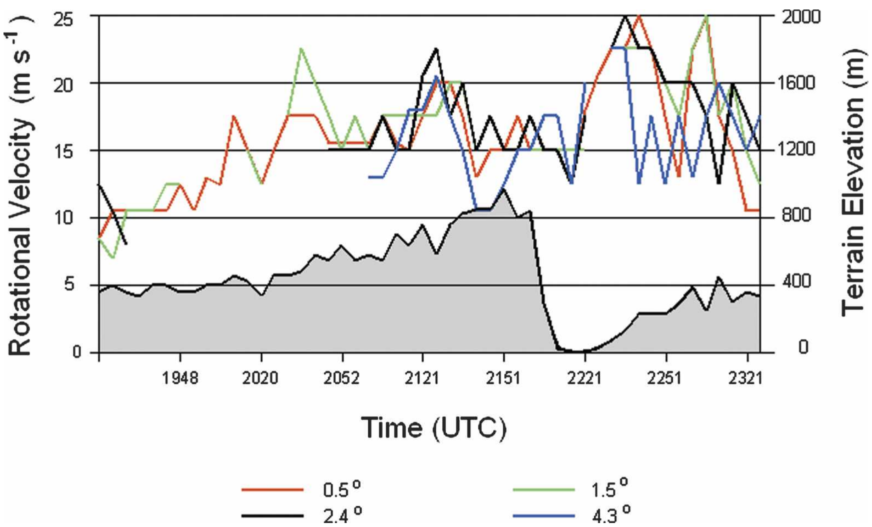

FIG. 10. Time series of radar-derived rotational velocity (m s^{-1}) from KBGM and KENX for the period 1913–2321 UTC 29 May 1995 at beam elevation scans of 0.5° (red), 1.5° (green), 2.4° (yellow), and 4.3° (blue). Shaded area indicates terrain elevation (m) along storm's path according to the scale at the right.

4. Developing supercell stage: 2000–2210 UTC 29 May 1995

The complexity of the GBR storm's evolution through the developing supercell stage prior to tornadogenesis requires a detailed analysis of the KENX radar observations and is discussed in this section. A series of 0.5° base reflectivity plots spanning the period 2141–2211 UTC 29 May shows the evolution of the developing GBR supercell (Fig. 11). At 2141 UTC a northeast–southwest broken line of storms extended from east-central Vermont southwest across the Catskills. An arcing line segment near the border of northwest Massachusetts and southwest Vermont produced a few severe weather reports (wind and hail). It was associated with the storms that crossed the ALB region after 2100 UTC (Fig. 8). The GBR supercell, associated with a second arcing line segment to the southwest over the eastern Catskills [just to the west of Tannersville, New York (TNR)], tracked eastward between 2057 and 2141 UTC (Figs. 9d and 11). The area of convection behind the outflow boundary northeast of the GBR supercell at 2057 UTC (Fig. 9d) was apparent behind a leading surge of weaker reflectivity values at 2141 UTC.

The GBR supercell began to split as it approached and moved off the Catskill escarpment (2141–2151 UTC 29 May) with the split quite apparent by 2211 UTC (Figs. 11b, 11c, 11d, and 12). The left-moving storm formed in northern Greene County on the northern flank of the GBR supercell and at the southern end of a gust front that was moving eastward across Albany County (Figs. 12 and 13, and Figs. 14b and 14c). Although the northern (left moving) storm was never associated with any reported severe weather (KENX radar loops revealed weak anticyclonic rotation, not shown), it intensified on the GBR supercell's northern flank from 2151 to 2201 UTC as it moved off the Catskill escarpment (Figs. 11b and 11c).

The dominant right-moving supercell that would spawn the GBR tornado continued to move east-southeast at ~17 m s^{-1} over the higher terrain of the Catskills. At 2201 UTC 29 May, the centroid of the GBR supercell was located over mountainous terrain at a mean elevation of over 900 m north of TNR and west of Cairo, New York (CAI). By 2211 UTC, the right-moving supercell was beginning to cross the Hudson River (Fig. 11d). Prior to storm-splitting (2121–2141 UTC) there was a general decrease in rotational velocities, especially at the 4.3° beam elevation angle where the decrease was almost 10 m s^{-1} (Fig. 10). However, beginning just after 2141 UTC, the rotational velocity began to increase at both the 0.5° and 4.3° beam elevation angles (Fig. 11a). This increase in rotational velocity occurred as the original supercell split with the right-moving storm becoming the GBR supercell. It was also consistent with the apparent strengthening and compaction of the reflectivity core in the GBR supercell by 2211 UTC (Fig. 11d).

By 2201–2211 UTC 29 May, the Hudson Valley region just to the north of the GBR supercell was enveloped by a solid area of 20–30-dBZ reflectivity values

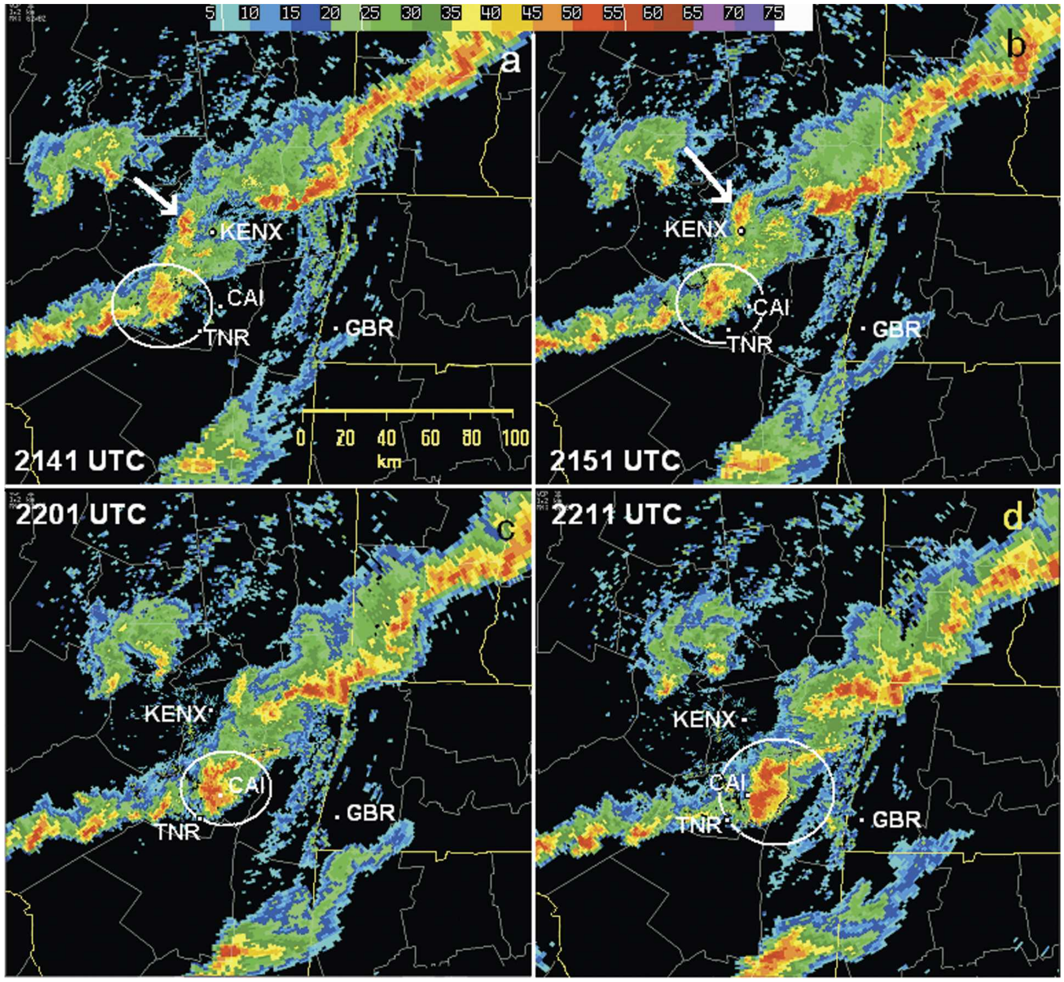

FIG. 11. Same as in Fig. 9 but at (a) 2141, (b) 2151, (c) 2201, and (d) 2211 UTC 29 May 1995 as obtained from the KENX radar from a 0.5° scan. White ovals indicate the location of the GBR storm and arrows in (a) and (b) indicate the area of convection behind the outflow boundary northeast of the GBR supercell.

with smaller embedded 35–50-dBZ reflectivity cores (Figs. 11c and 11d). A small, narrow band of enhanced 40–45-dBZ reflectivity cores, situated just to the east-northeast of the left-moving storm from 2201 to 2211 UTC, was near the leading edge of a second general precipitation area (20–30-dBZ reflectivity values) that was approaching the Hudson River valley near the mouth of the Catskill Creek (Figs. 11c and 11d). The Catskill Creek is oriented northwest–southeast and has a small (5–10 km) opening in the eastern Catskills escarpment where it leads into the Hudson Valley (Figs. 1c and 2). The enhanced reflectivity cores in the small band ahead of the left-moving storm were located near the mouth of the Catskill Creek. Although this juxtaposition of enhanced radar echoes with the mouth of the Catskill Creek was most likely coincidental, the possibility that a portion of the convectively driven cold outflow air from storms to the northeast of the GBR supercell spilled down the Catskill Creek cannot be ruled out (cf. Fig. 9d with Figs. 11a, 11b, and 11c). Overall, the GBR supercell strengthened as it approached the Hudson River and began to interact with the larger-scale outflow by 2211 UTC (Fig. 11d). At issue is whether any of the cold outflow air that may have spilled down the Catskill Creek could have contributed to the strengthening through enhanced low-level convergence near the GBR supercell as it moved off the Catskill escarpment.

To address this issue a series of base velocity maps during the initiation of the tornadic phase of the GBR supercell for the period 2121–2201 UTC 29 May are presented (Fig. 12). Two separate regions of 20 m s^{-1} inbound air over western Schoharie County, New York, at 2102 UTC 29 May (not shown) coalesced into one large inbound surge over central Schoharie County by 2121 UTC (Fig. 12a) and reached

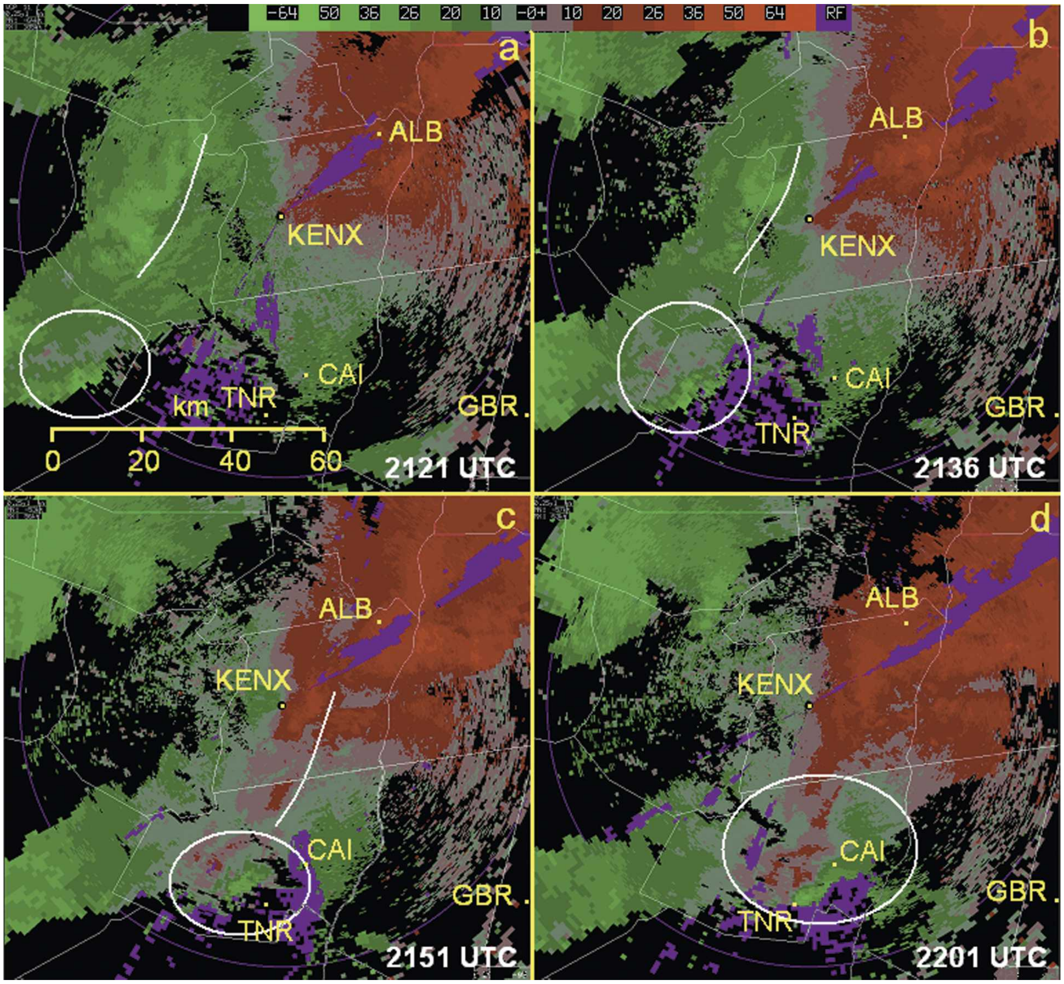

FIG. 12. KENX radar base velocity maps from a 0.5° scan at (a) 2121, (b) 2136, (c) 2151, and (d) 2201 UTC 29 May 1995. Warm (cool) colors denote outbound (inbound) velocities (kt) scaled according to the color bar. White ovals indicate location of GBR storm and white solid lines indicate position of the gust front.

extreme western Albany County by 2136 UTC (Fig. 12b). This region of relatively large inbound velocities (gust front) was associated with the left-moving storm and other convection to the north of the GBR supercell, which was located to the southwest of the gust front (Figs. 11a and 12b). The weak left-moving storm was rotating anticyclonically and was located at the southern end of the eastward-moving gust front. The leading edge of the gust front was near KENX at 2136 UTC (Fig. 11b) and between 2136 and 2201 UTC it moved downslope out of the Catskills into the western side of the Hudson Valley (Figs. 12b, 12c, and 12d). A portion of the gust front enveloped the Catskill Creek as it approached the Hudson Valley. From 2206 to 2211 UTC the right-moving storm (GBR supercell) crossed the steep eastern Catskills escarpment and entered the Hudson Valley (Fig. 11d). At 2216 UTC the GBR supercell was located near the southern end of the Catskill Creek at an elevation of $<$200 m, a net terrain height reduction of $>$700 m in 15 min (not shown). An isochronal analysis of the leading edge of the cold outflow surge constructed from the KENX base velocity observations showed that the surge intercepted the GBR supercell as it reached the Hudson Valley after descending the Catskill Creek (Fig. 13). Based on these observations, an initial (speculative) inference is made that cold outflow from the north moved down the Hudson Valley where it was reinforced in part by additional outflow that descended the Catskill Creek. Extrapolation of the movement of the cold outflow showed that it was in a position to be intercepted by the GBR supercell as it reached the mouth of the Catskill Creek and entered the Hudson Valley (Fig. 13).

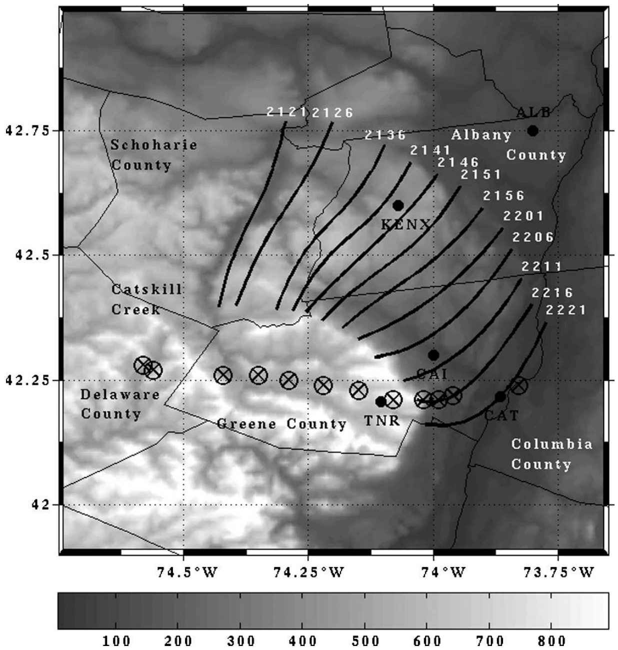

FIG. 13. Isochrones of the leading edge of the Catskill Creek outflow boundary surge and position of the reflectivity core of the GBR storm on 29 May 1995 (marked by encircled x symbols) for UTC times given. Note that the outflow boundary is far more extensive than the Catskill Creek Valley.

5. Pretornadic supercell stage: 2210–2230 UTC 29 May 1995

The pretornadic supercell stage coincided with the GBR supercell's interaction with the cold outflow surge down the Hudson Valley (and the Catskill Creek) and the terrain-channeled southerly flow up the Hudson Valley. To help bolster our inference about the cold outflow surge behavior, note that weak outbound flow (approximately 5–10 m s^{-1}) was evident over the region north of CAI that included the Catskill Creek from 2206 to 2211 UTC 29 May (Figs. 14a and 14b). A separate reflectivity core with a low-level 15–20 m s^{-1} differential velocity rotation was located to the north of the GBR supercell rotational velocity couplet at 2206 UTC (Fig. 14a). This feature, more apparent at 2211 UTC, moved northeastward, away from the larger, right-moving GBR supercell (Figs. 14a and 14b). A separate and distinct rotational velocity couplet (~20 m s^{-1} over 12 km) that moved off the Catskill escarpment east of TNR toward the southern end of the Catskill Creek could be associated with the GBR supercell from 2206 to 2211 UTC (Figs. 14a and 14b).

By 2216 UTC 29 May, the eastward-moving GBR supercell was positioned so that the inbound velocity maximum (~15 m s^{-1}) lay over the town of Catskill, New York (CAT), at the southern end of the Catskill Creek (Fig. 14c). The corresponding outbound velocity maximum (~10 m s^{-1}) was still 10–15 km to the west over the Catskill escarpment. More importantly, a second outbound velocity maximum (>15 m s^{-1}) appeared within an area that included the southern end of the Catskill Creek valley, ~10 km northwest of the inbound velocity maximum associated with the GBR supercell (Fig. 14c). This second outbound velocity maximum was in the process of intercepting the GBR supercell (Fig. 13). Five minutes later (2221 UTC) this outbound velocity maximum (>15 m s^{-1}) had increased in areal extent and had moved to within 6 km of the inbound velocity maximum associated with the GBR supercell (Fig. 14d). Between 2211 and 2221 UTC the areal extent of the inbound velocity maximum >20 m s^{-1} was reduced by almost 50% while its magnitude remained unchanged (Fig. 14d).

The observed compaction of the GBR supercell inbound–outbound velocity couplet coincided with the arrival of the leading edge of the cold outflow surge in the northwest periphery of the mesocyclone (Fig. 14d). The original outbound velocity maximum associated with the GBR supercell remained to the west of the new inbound–outbound velocity couplet and did not strengthen (Figs. 14c and 14d). An estimated rotational velocity difference of ~23 m s^{-1} over a 10-km diameter in the original mesocyclone increased to ~31 m s^{-1} over a 6-km diameter in 10–15 min as the compacting GBR supercell moved off the Catskill escarpment and interacted with the advancing cold outflow boundary to the north and northwest. The observed increase in rotational velocity computed for all beam elevation scans between 2221 and 2236 UTC lends support to this assertion (Fig. 10). Of obvious interest is whether the cold outflow air from the north and northwest was buoyant enough to fuel the mesocyclone updraft when it encountered the GBR supercell. The authors are unaware of any observations that could be used to document the thermodynamic characteristics of the more general outflow interacting with the GBR storm as well as outflow associated with the storm itself.

In an effort to better assess the observed change in structure of the GBR supercell as it moved off the higher elevations of the Catskills into the lower elevations of the Hudson Valley, a combined base reflectivity, composite reflectivity, and base velocity analysis was constructed (Fig. 15). The 50-dBZ threshold is used for the base and composite reflectivities. At 2211 UTC 29 May, an inbound velocity maximum >18 m s^{-1} was located near the southern edge of the GBR supercell (Fig. 15a). As the GBR supercell moved eastward across the Hudson River, the inbound velocity maxi-

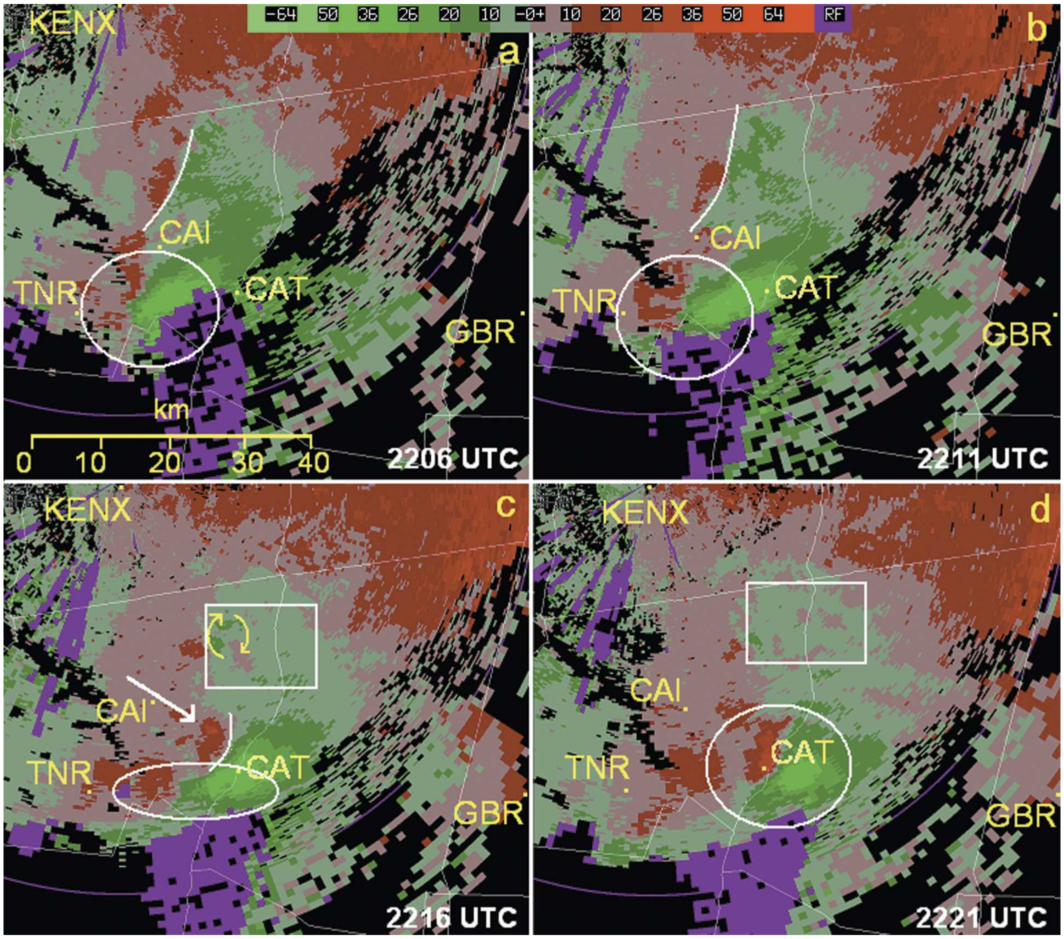

FIG. 14. Same as in Fig. 12 but at (a) 2206, (b) 2211, (c) 2216, and (d) 2221 UTC 29 May 1995. White ovals indicate location of GBR supercell, white rectangles indicate location of left-moving cell with anticyclonic rotation noted at 2216 UTC, and solid white line indicates location of gust front.

mum tended to remain in the same storm-relative position, suggestive that it was responding to the storm updraft (Fig. 15). At 2211 UTC (Fig. 15a) the inbound velocity contour >13 m s^{-1} subtended an area extending to the west-southwest and east-northeast of the inferred updraft location. The inbound velocity maximum was identified by a (yellow) pixel of >18 m s^{-1} inflow that was located to the south-southeast (upstream from the perspective of the channeled low-level flow up the Hudson Valley) of the updraft core (based on the 50-dB*Z* composite and base reflectivity contours; at the observed distance of the GBR supercell from KENX, the inbound velocity components are representative of ~1 km above the surface) (Fig. 15a).

Also of interest was the change in shape of the inbound velocity maximum as the GBR supercell traversed the Hudson Valley. At 2211 UTC 29 May, while the GBR supercell was still west of the Hudson River, the inbound velocity maximum was oriented northeastward, quasi-parallel to the downshear anvil precipitation immediately to the north (Fig. 15a). By 2221 UTC, when the GBR supercell was crossing the Hudson River, the inbound velocity maximum was more compact and situated to the south-southeast of what appeared to be a reflectivity notch (Figs. 15b and 15c). At this time the radar-derived rotational velocities had just started to increase, from which we infer that the observed compaction of the inbound velocity maximum possibly marked the start of the intensification of the GBR mesocyclone (cf. Figs. 10 and 15c). The observed orientation of the inbound velocity maximum may also indicate the establishment of a strong boundary where outflow from the north (Catskill Creek and Hudson Valley) and the forward-flank downdraft met terrain-channeled inflow from the south. While the observations are insufficient to determine if this inference could be correct, such a boundary, if present, would provide a rich source of horizontal vorticity that could

FIG. 15. Combined KENX 0.5° base reflectivity, composite reflectivity, and base velocity at (a) 2211, (b) 2216, and (c) 2221 UTC 29 May 1995. Red-shaded areas indicate base reflectivity values >50 dBZ. Black dashed lines enclose areas of composite reflectivity >50 dBZ. Green (yellow) shading denotes areas of inbound velocities of 13–18 m s^{-1} (18–25 m s^{-1}). The KENX radar is located in the upper portion of each image. The Hudson River runs along the border of Greene and Columbia Counties.

be subsequently tilted into the vertical and/or preexisting vertical vorticity within the outflow that could be subsequently stretched where it was ingested into the updraft region of the approaching mesocyclone as is typical storm behavior of supercells observed elsewhere (e.g., Weisman and Rotunno 2000; Davies-Jones et al. 2001; Wilhelmson and Wicker 2001). Finally, a subjectively analyzed cross section through the GBR supercell at 2216 UTC (time of Fig. 15b) established that inbound velocities were >20 m s^{-1} below 2 km just ahead of the reflectivity tower and outbound velocities were >5 m s^{-1} below 1.5 km in the core of the reflectivity tower (Fig. 16). The updraft is likely located near the front (right side in Fig. 16) of the reflectivity core (near the gradient) and probably above the strong convergence.

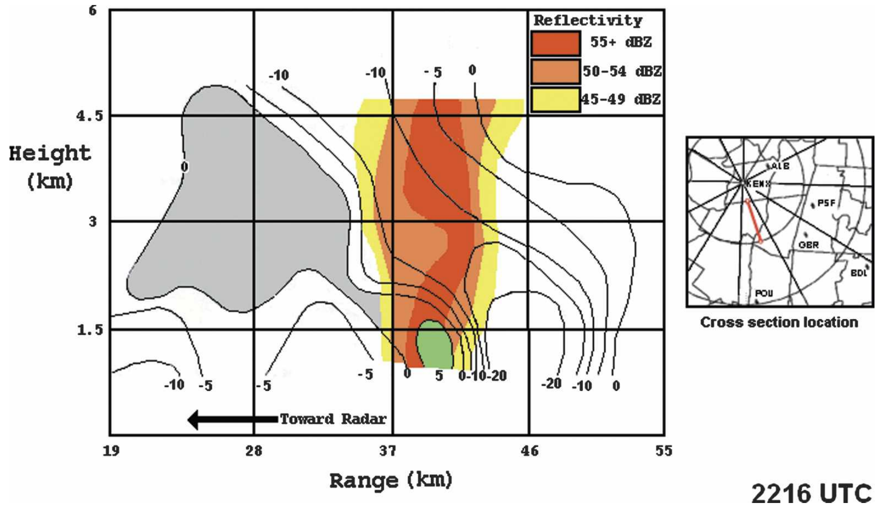

FIG. 16. Manually constructed cross section of the GBR storm at 2216 UTC 29 May 1995 as the storm moved into the Hudson Valley as derived from the KENX radar base reflectivity and storm-relative velocity observations. Red, orange, and yellow shading denote base reflectivities >55, 50–54, and 45–49 dBZ, respectively. Solid lines indicate storm-relative velocity values with negative (positive) values toward (away) from the radar. Outbound storm-relative velocities >5 m s^{-1} (0–5 m s^{-1}) are shaded green (gray).

6. Tornadic supercell in the Hudson Valley and Berkshires: 2230–2330 UTC 29 May 1995

A time series of the inbound–outbound shear across the GBR mesocyclone as derived from an average over the three lowest elevations scans (0.5°, 1.5°, and 2.4°) of the KENX radar along the mesocyclone track is used to summarize the results of section 5 and set the stage for the tornadic phase of the GBR supercell in the Hudson Valley (Fig. 17). Immediately after 2200 UTC 29 May there was a rapid decrease in terrain height from ~800 m to <200 m as the GBR supercell moved off the eastern Catskills escarpment and entered the Hudson Valley. Beginning at 2216 UTC and continuing until 2231 UTC, the average inbound–outbound shear increased slowly from 0.005 to ~0.013 s^{-1} while the storm was in the Hudson Valley. This was followed by a much more abrupt average shear increase to 0.05 s^{-1} in the 15-min period ending at 2246 UTC as the mesocyclone ascended the higher terrain to the east of the Hudson Valley and intensified (Fig. 17). The increase in average inbound–outbound shear corresponded to the first tornadic phase of the GBR supercell as the storm crossed Columbia County, New York, immediately to the east of the Hudson River.

The storm-relative base velocity data at 2221 UTC 29 May showed a well-defined mesocyclone, but without a tornado vortex signature (TVS; Brown et al. 1978; Trapp et al. 1999) at both the 0.5° and 4.3° beam elevation scans (Figs. 18a and 19a, respectively). The corresponding base reflectivity data at the 0.5° scan for 2221 UTC showed a broad area of 35 dBZ and greater echo coverage along the border of Greene and Columbia Counties in New York (Fig. 20a). The GBR supercell, with a developing hooklike appendage on its southwest side, was situated in the central portion of this high-reflectivity area. A weak-echo region (<35 dBZ) to the east of the developing hook echo (0.5° scan) was under a region of higher reflectivities (4.3° scan), possibly

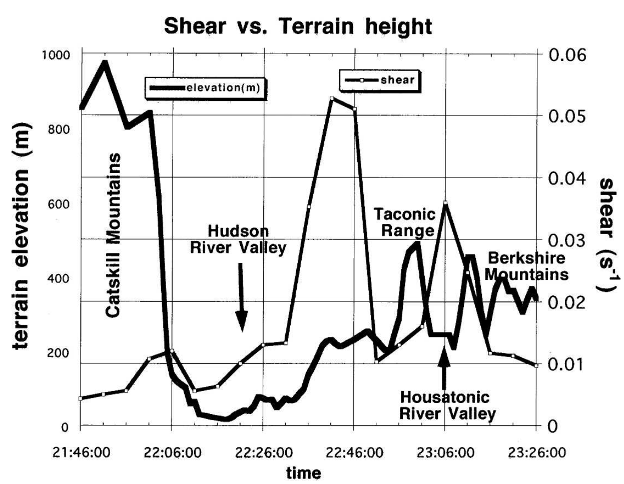

FIG. 17. Inbound–outbound shear (s^{-1}; solid) derived from KENX WSR-88D volume scans averaged over the lowest three elevation scans (0.5°, 1.5°, and 2.4°) along the disturbance path from 2146 to 2326 UTC 29 May 1995. Terrain elevation (m) shown as a solid, thick black line with key topographic landforms labeled.

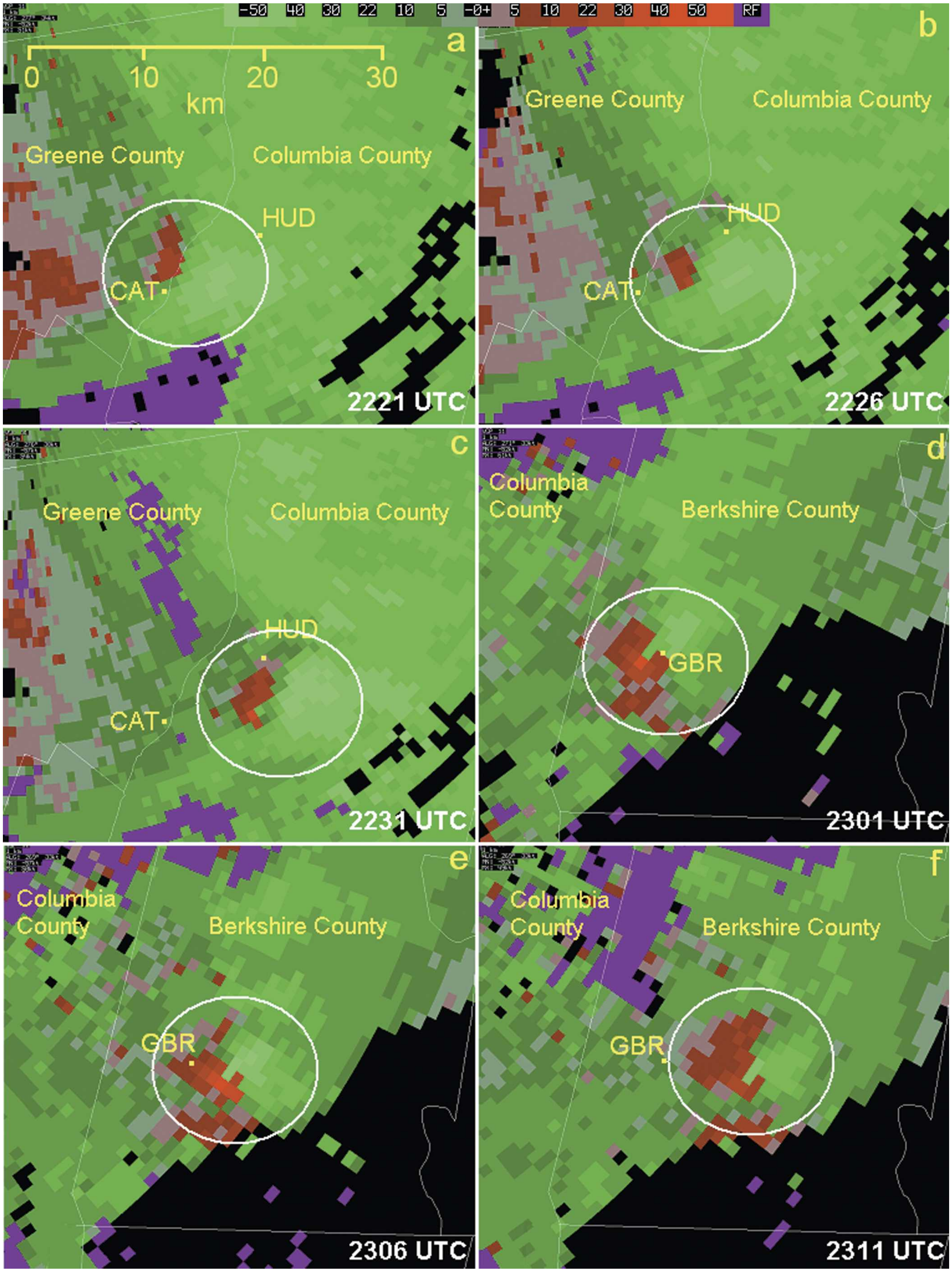

FIG. 18. KENX storm-relative velocity maps (1000-m resolution) from a 0.5° beam elevation scan at (a) 2221, (b) 2226, (c) 2231, (d) 2301, (e) 2306, and (f) 2311 UTC 29 May 1995. The location of the KENX radar is in the upper-left corner of each image. Velocity units in kt scaled according to the color bar. White ovals indicate the location of the GBR supercell and mesocyclone.

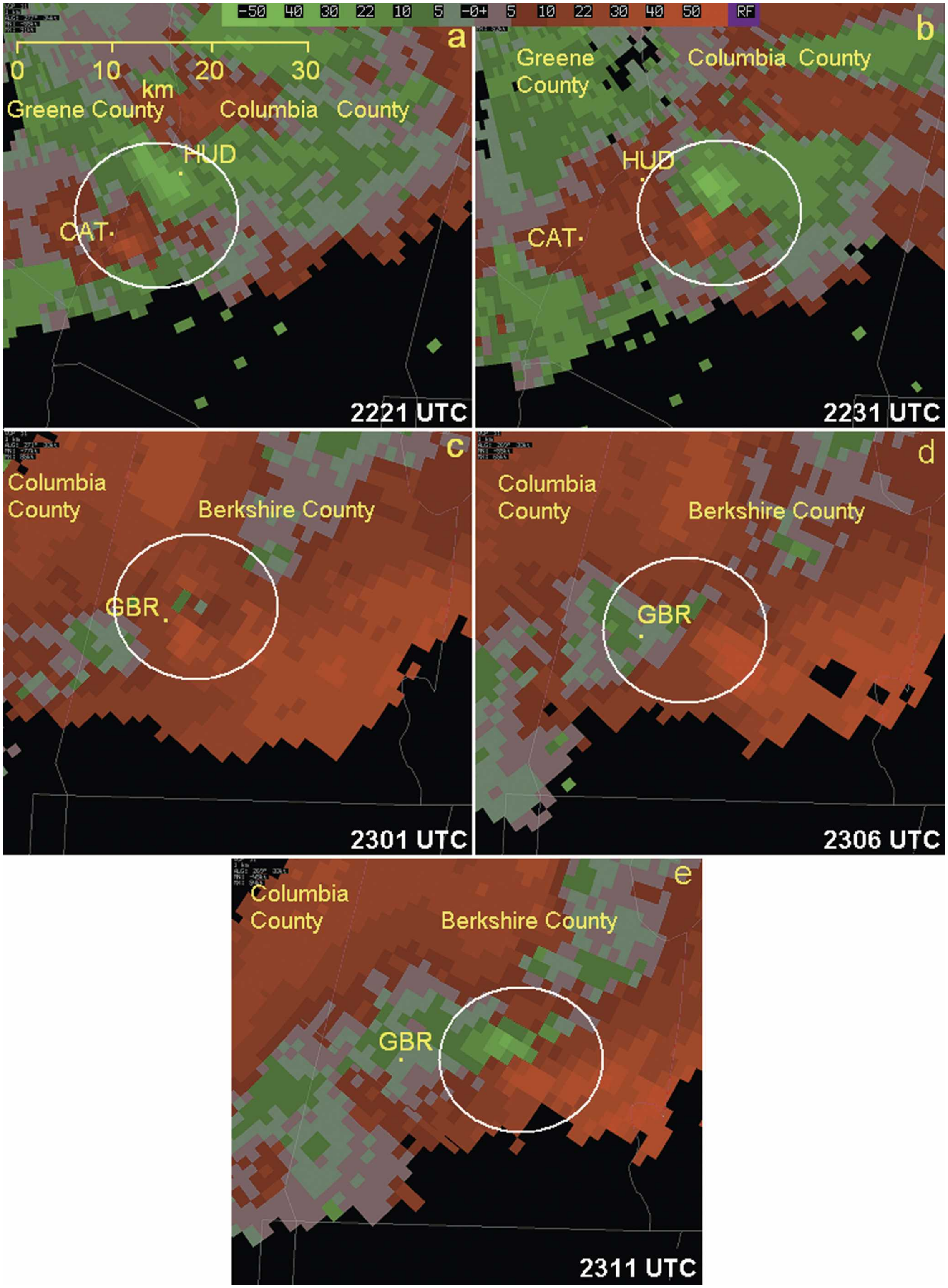

FIG. 19. Same as in Fig. 18 but from a 4.3° beam elevation scan with no image at 2226 UTC.

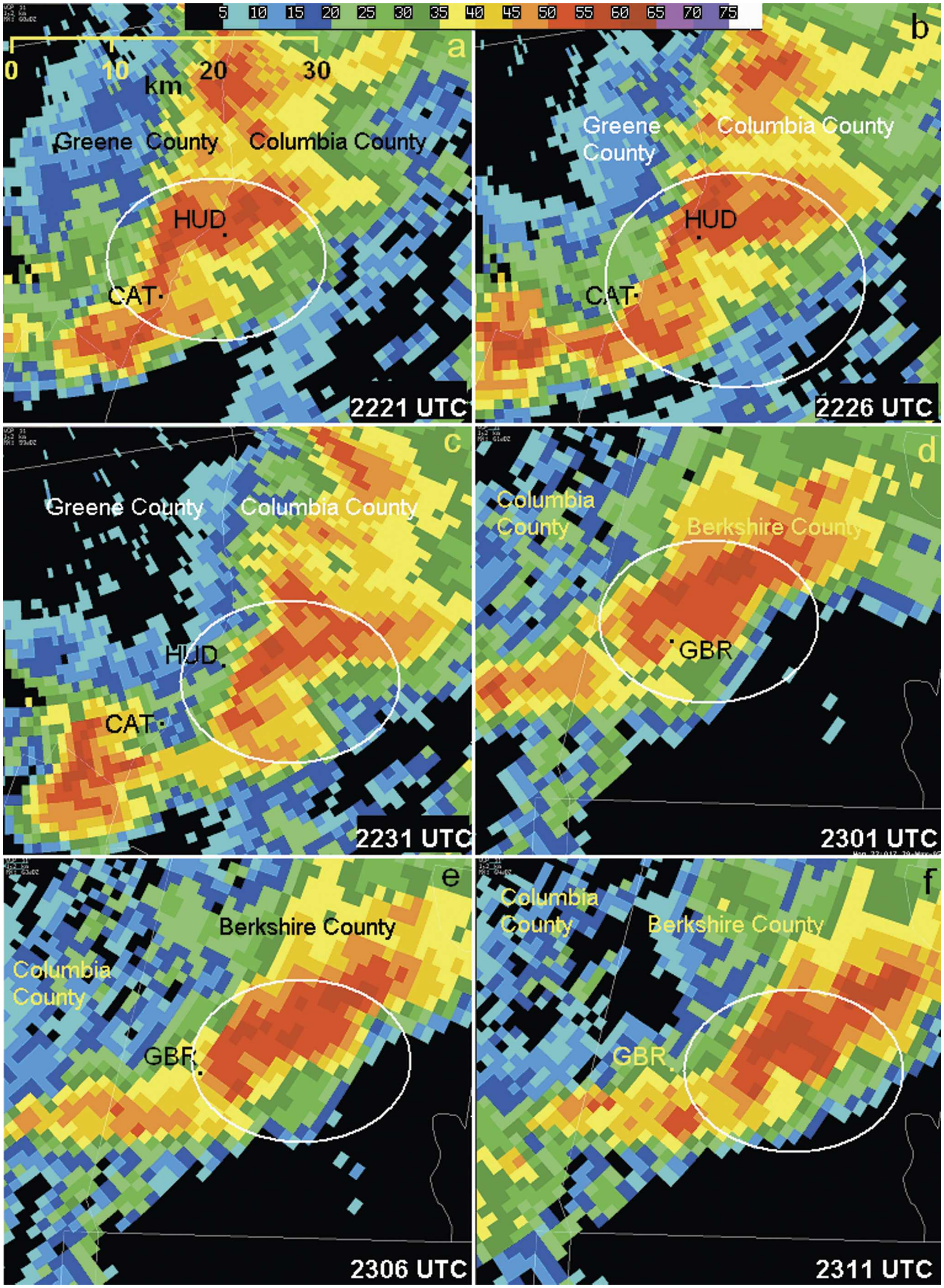

FIG. 20. Same as in Fig. 18 but for base reflectivity (dBZ).

indicative of a bounded weak echo region (BWER) (Figs. 20a and 21a).

Although the exact time of tornado development in Columbia County was unknown, an aerial damage survey on 31 May 1995, in which two of the authors participated, indicated that the origin of a major tornadic damage swath was 5 km due east of CAT.[1] By 2226 UTC 29 May, a well-defined intensifying mesocyclone was apparent on both the 0.5° and 4.3° storm-relative velocity scans (Figs. 18b and 19b, respectively). The corresponding 0.5° and 4.3° base reflectivity scans clearly exhibited a relatively conventional supercellular structure with a pronounced hook echo on the southwest side of the supercell (Figs. 20b and 21b). The intensifying mesocyclone and hook echo were situated ~5 km east of CAT, near the beginning of the observed damage path (Fig. 20b). Between 2226 and 2231 UTC, the KENX radar showed the development of a TVS structure in the 0.5° and 4.3° storm-relative velocity data (Figs. 18b and 18c, and Figs. 19b and 19c, respectively) and the formation of a hook echo in the 0.5° base reflectivity data (Figs. 20b and 20c) below the BWER in the 4.3° scan (Figs. 21b and 21c). Between 2231 and 2241 UTC, the tornadic mesocyclone reached its peak intensity as it crossed the Hudson Valley and ascended the low (~250 m) western foothills of the Taconic Range (Figs. 2, 10, and 17). Between 2241 and 2251 UTC, this mesocyclone weakened slightly, then significantly, in advance of the ~600 m crest of the Taconic Range (Figs. 2, 10, and 17). The radar-indicated weakening of the tornadic mesocyclone west of the Taconic Range coincided with the end of the tornado's damage path before it reached the highest terrain of the Taconic Range west of GBR (Figs. 1b, 1c, and 2).

Between 2301 and 2306 UTC 29 May, the inbound–outbound shear across the GBR mesocyclone increased and the tornadic mesocyclone, associated hook echo, and BWER all became better defined as the storm entered the Housatonic Valley (Figs. 10, 17, 18e, 19d, 20, and 21e). At about this time, a second tornadic damage path began in far western Massachusetts and continued eastward toward the south side of GBR (Fig. 1c). By 2311 UTC the tornado, after causing devastation and fatalities in GBR, weakened again as it moved upslope over the higher terrain to the east of the Housatonic Valley (Figs. 18–21f). Subsequently, the mesocyclone, hook echo, and BWER continued to slowly weaken as the storm entered the Berkshires. The damage track ended near West Otis, Massachusetts (WOT), at about 2325 UTC. Although the storm continued to move east across Massachusetts, it never produced another documented tornado.

[1] See Grazulis (1997) for additional documentation of this storm.

7. Concluding discussion

It is impossible to know what transpired when the GBR supercell descended the eastern Catksills, entered the Hudson Valley, intensified, and then underwent tornadogenesis. The available (limited) evidence suggests an interesting and perhaps unconventional storm evolution that implicates terrain interactions in tornado formation. The absence of direct surface and upper-air observations and detailed radar-derived wind observations on time scales of less than 5 min severely hampers our ability to resolve the temporal evolution of the tornadogenesis process and to quantify a possible cause and effect. Given these significant analysis limitations, but mindful of the apparent rarity of significant tornadogenesis in rough terrain from a supercell well documented in operational Doppler radar data, an attempt has been made to relate supercell thunderstorm evolution, inferred primarily from Doppler radar reflectivity and velocity patterns, to underlying landform characteristics in the near-storm environment.

Although the analysis in the absence of detailed mesoscale observations was necessarily limited, the results suggest that orogenic channeled flows may have been important components in the mesoscyclone intensification and tornadogenesis. The GBR supercell possessed a midlevel mesocyclone while it was located to the west of the Catskill Mountains and well before tornadogenesis. Rotational velocities in the GBR storm at the three lowest radar beam elevation angles (0.5°, 1.5°, and 2.4°) were ~10 m s^{-1} over 10 km as early as 1913 UTC 29 May (~3 h before tornadogenesis) while the storm was still well west of the Catskills. Over the next hour the radar-derived rotational velocities increased to ~15 m s^{-1} as the GBR storm reached the western Catskills and the KENX radar first detected a mesocyclone at 2000 UTC. As the line of thunderstorms containing the GBR supercell became better organized, a new thunderstorm developed 15–20 km to the northeast of the GBR supercell. This second storm maintained its identity as it crossed the northern Catskills. At the same time the GBR supercell split. The left-moving (northern) cell assumed its own identity with a distinct reflectivity core and a weak anticyclonic rotation. Both the new convection and the left-moving storm were instrumental in generating outflow boundaries that eventually interacted with the GBR supercell.

Our analysis revealed that the GBR mesocyclone

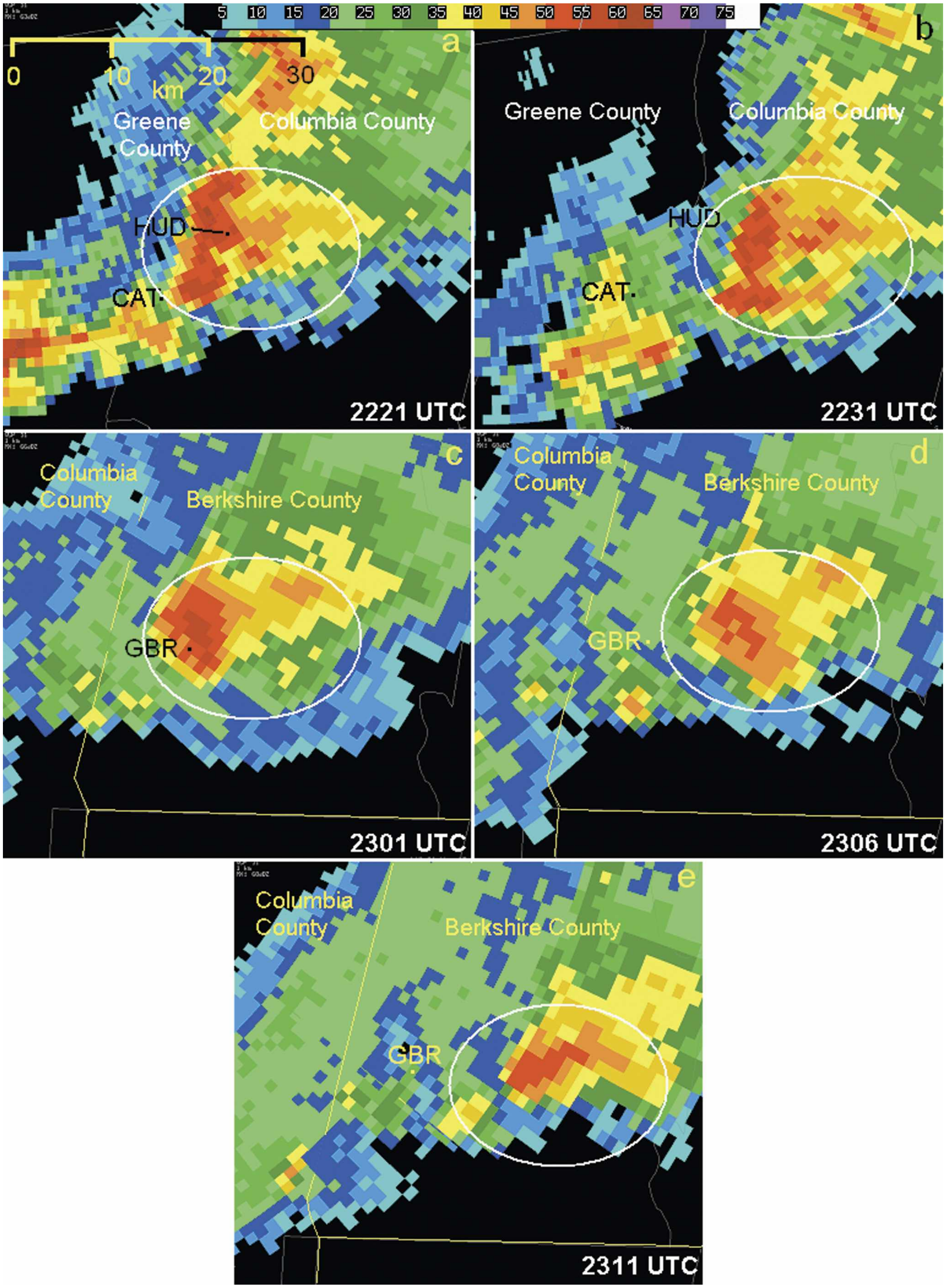

FIG. 21. As in Fig. 20 but from a 4.3° beam elevation scan with no image at 2226 UTC.

compacted and intensified, and the rotation rate increased as it moved off the eastern end of the Catskill escarpment and entered the Hudson Valley. The observed change in the structure of the GBR mesocyclone also coincided with the arrival of a cold outflow surge from the north down the Hudson Valley and likely from the northwest down the topographic trough that marked the Catskill Creek and into the Hudson Valley. On the basis of observations from KENX, this combined outflow surge appeared to be triggered by new convection that formed to the northeast of the GBR supercell and was reinforced by outflow from the left-moving (northern) weak anticyclonically rotating cell that originated from the observed split of the GBR supercell. The combined outflow surge also appeared to be intercepted by the GBR supercell as it descended the eastern Catskill escarpment and entered the Hudson Valley near the mouth of the Catskill Creek. Independent surface mesoscale observations necessary to verify the existence, evolution, structure, and thermodynamic characteristics of the outflow surge and to quantify the environmental low-level (channeled) southerly flow characteristics in the Hudson Valley near the mouth of the Catskill Creek were unavailable. Despite this limitation, the available radar data suggests that the structure of the GBR mesocyclone evolved as it encountered a change in terrain slope beneath it and a new low-level environment in the Hudson Valley. Subsequently, the GBR mesocyclone 1) slowly intensified as it crossed the Hudson River valley, 2) strengthened rapidly and became tornadic as it ascended the low ($\sim$250 m) highlands east of the Hudson River, 3) weakened rapidly as it approached the western slopes of the Taconic Range in extreme western Massachusetts, and 4) intensified again as it moved downslope into the Housatonic Valley where it was associated with the GBR tornado.

The most important factor in the observed intensification of the GBR mesocyclone and ensuing tornadogenesis was the existence of a terrain-channeled low-level (0–1 km) southerly flow in the Hudson Valley as determined directly from ALB surface observations and indirectly from the KENX inbound velocity data. As the result of this terrain-channeled southerly flow, the wind hodograph in the Hudson Valley was lengthened relative to that over the higher terrain of the Catskills to the west. The associated enhanced veering wind profile in the lowest 1 km and increased storm-relative helicity and shear have been shown to favor low-level mesocyclone development and tornadogenesis, assuming the large-scale environment is favorable for supercell formation, in idealized modeling studies (e.g., Wicker et al. 1996; Wicker 2000; Wilhelmson and Wicker 2001).

Recent studies using the National Centers for Environmental Prediction's (NCEP) Rapid Update Cycle model-generated proximity soundings (Thompson et al. 2003) and observed proximity soundings (Rasmussen 2003) suggest that shear and storm-relative helicity in the 0–1-km AGL layer are better at discriminating supercells that produce significant tornadoes from nontornadic supercells than deep-layer (0–6-km shear and 0–3-km storm-relative helicity) measures of these parameters. Terrain-channeled southerly flow in the Hudson Valley is a common signature in station (e.g., ALB) surface wind rose climatologies (e.g., Wasula et al. 2002; LaPenta et al. 2005). Other significant tornado weather events in the Northeast, including the 31 May 1998 Mechanicville, New York, F3 tornado in the Hudson Valley (LaPenta et al. 2005) and the 3 October 1979 Windsor Locks, Connecticut, F4 tornado in the Connecticut Valley (Riley and Bosart 1987), have featured terrain-channeled low-level southerly flow and enhanced low-level wind veering. That said, the issue of how terrain-channeled flow up the Hudson Valley influences where the tornadogenesis occurs after the GBR supercell exits the Hudson Valley remains unresolved and is a subject for future research.

Our analysis also raised several issues that are unable to be addressed because of the absence of critical observations. One issue is whether the observed acceleration of the low-level southerly flow up the Hudson Valley was induced by the updraft of the GBR supercell (a positive feedback factor involving the supercell's pressure fall center) and/or was produced by the terrain-channeled low-level southerly flow. An argument for updraft-related gradient and/or isallobaric acceleration was that the radar-derived inbound velocity maximum appeared to be associated with the GBR storm in that as the storm moved eastward across the Hudson River the inbound velocity maximum tended to remain in roughly the same storm-relative (inflow) position. An argument for terrain-channeled low-level southerly flow acceleration was that the radar-indicated inbound velocity maximum subtended an area extending both upstream and downstream of the inferred updraft location. It would be difficult to explain the presence of a strong radar-relative inbound velocity maximum in the wake of the mesocyclone when this velocity maximum extended behind the mesocyclone as it did in this case (e.g., Weisman et al. 1998). A second issue is whether the initial intensification of the GBR mesocyclone responded to the changed thermodynamic environment resulting from the ingestion of higher-θ_e inflow air in the Hudson Valley. Observations are lacking to provide detailed mesoscale surface and temporal resolution in the Hudson Valley and adjacent mountain regions. A third issue is whether the rapid decrease in boundary layer friction as the mesocyclone encountered the broad Hudson Valley after experiencing the enhanced roughness of the Catskills contributed in any way to the radar-indicated changes in mesocyclone structure. It is speculated that all three issues might be important to mesocyclone intensification and tornadogenesis, but only as supporting actors to the more significant topographic channeling effects. Future modeling studies are recommended to quantify and sort out the competing possibilities.

The observed elongated radar-relative inbound velocity maximum was probably mostly orogenic and the observed eastward propagation of the peak inbound velocity maximum through it was likely a manifestation of the intensifying updraft and associated gradient and/or isallobaric acceleration. Evidence for or against this assertion should also be sought in numerical modeling studies. The observed acceleration of the radar-relative inbound wind maximum was probably a product of the GBR supercell interacting with the Catskill escarpment, not just one or the other. The observed radar-relative outbound wind maximum that developed along the Catskill Creek was perhaps produced by the channeling of part of the outflow from the thunderstorm reflectivity core region down the Catskill Creek topographic trough into the Hudson Valley. Similarly, the observed elongated radar-relative inbound velocity maximum was probably mostly orogenic and the observed eastward propagation of the peak inbound velocity maximum through it was probably a manifestation of the intensifying updraft and associated gradient and/or isallobaric acceleration. In this regard, the behavior of these channeled flows and resultant tornadogenesis may have been predicated by the chance movement of the GBR supercell across the complex, but highly defined, topographic domain of the Catskills.

Significant tornadoes over the Northeast are rare as compared with the Great Plains and this difference cannot be attributed solely to terrain roughness variations. CAPE values tend to be larger more often over the plains, given the steeper midlevel lapse rates in the warm season associated with the eastward movement of elevated mixed layers off the Rockies and the more infrequent incursions of warm, moist air from the Gulf of Mexico. Similarly, days with large shear and large CAPE are less common in the Northeast than in the plains because low-level southerly flow ahead of migratory troughs often has a trajectory off the cooler waters of the Atlantic, especially east of the Appalachians and earlier in the warm season. When severe weather outbreaks occur east of the Appalachians, especially from Pennsylvania southward, a lee trough is often present east of the mountains. Backed low-level winds ahead of the lee trough can act to lengthen the hodographs in these situations.

These differences aside, the occasional development of large, intense, and long-lived tornadoes over rough terrain has not been explained to date. Our understanding is that it takes a deeper mesocyclone with strong dynamical forcing to get a significant tornado over mountainous terrain. Analysis of the GBR supercell and its associated tornadoes has provided insight on some factors that are possibly responsible for setting these rare events apart from other mountain area convective phenomena. A mesoscale environment supportive of supercell thunderstorm development according to conventional indicators of wind shear and static stability is sufficient to spawn a supercell above mountainous terrain, but significant tornadogenesis is unlikely to ensue unless local modifications to the low-level wind field are present to increase the vorticity and convergence at spatial scales similar to that of the supercell itself. Topographic configurations such as valley confluences appear to offer local orographic enhancements to tornadogenesis potential to compensate for the disruptive influence of increased friction, but such interactions are dependent upon the channeling of ambient low-level flows and the specific propagation vector of a supercell. Analysis of other events at comparable spatial and temporal detail to that offered in this study will be required in order to establish more definitively how significant the orographic contributions to tornadogenesis are in complex terrain environments.

A critical factor for tornadogenesis is how a concentration of low-level cyclonic vorticity can be achieved in complex terrain. An external influence on a supercell mesocyclone crossing complex terrain may be needed to enable rapid mesoscale vertical vorticity growth. We speculate that the outflow surge down the Hudson Valley, a portion of which descended the Catskill Creek, may have played the role of an external influence on the GBR supercell. The chance juxtaposition of the Catskill Creek portion of the outflow surge with a channeled south-southeasterly flow up the Hudson Valley at the time the GBR supercell mesocyclone crossed the eastern escarpment of the Catskills may have helped to concentrate low-level vorticity ahead of the eastward-moving GBR supercell mesocyclone. It is possible that this surge introduces considerable angular momentum as well as cyclonic shear, on its southeastern side, into the near-surface environment beneath a strong, deep, and intensifying mesocyclone. In this context, the surge, which may have been serendipitous, may play a role similar to the rear-flank downdraft in "conventional" tornadogenesis in developing low-level mesocyclone rotation except that the surge is external to the mesocyclone. Numerical experimentation is needed to address these speculative points and related issues raised by this case study.

Acknowledgments. We extend thanks to Morris Weisman for his insightful comments on an earlier draft of this manuscript; to Ed Bracken for contributing to the storm analysis; Mitch Wemple for flying two coauthors (Bosart and Seimon) on aerial damage surveys; Peter O'Brien of Richmor Aviation for providing the crucial AWOS observations from the Columbia County airport; Daniel O'Brien of the New York State Emergency Management office for providing the GIS terrain profile; Jeff Waldstreicher of the NWS for providing a summary of storm behavior in the Binghamton, New York, region; and the reviewers for their constructive comments and suggestions. Celeste Iovinella is thanked for technical assistance and preparing the manuscript in final form. Conversations with Howie Bluestein, Chuck Doswell, Don Burgess, and Harold Brooks on the topic of tornadogenesis are appreciated. This research was supported by COMET Partners Program Grant NA37WD0018-01 to Lance Bosart at the University of Albany/SUNY and Kenneth LaPenta at the Albany, New York, NWS Forecast Office. Research support was also provided by National Science Foundation Grant ATM-9612485.

REFERENCES

Blier, W., and K. A. Batten, 1994: On the incidence of tornadoes in California. *Wea. Forecasting,* **9,** 301–315.

Bluestein, H. B., 2000: A tornadic supercell over elevated, complex terrain: The Divide, Colorado, storm of 12 July 1996. *Mon. Wea. Rev.,* **128,** 795–809.

Brotzman, W. S., 1944: Report of tornadoes of June 23, 1944 in Maryland, eastern Ohio, western Pennsylvania, and northern West Virginia. U.S. Weather Bureau, Pittsburgh, PA, 12 pp.

Brown, R. A., L. R. Lemon, and D. W. Burgess, 1978: Tornado detection by pulsed Doppler radar. *Mon. Wea. Rev.,* **106,** 29–38.

Costa, S., P. Mezzasalma, P. P. Alberoni, and V. Levizzani, 2000: Mesoscale and radar analysis of the 30 June 1998 supercell. *Phys. Chem Earth,* **25B,** 1289–1291.

Davies-Jones, R., R. J. Trapp, and H. B. Bluestein, 2001: Tornadoes and tornadic storms. *Severe Convective Storms, Meteor. Monogr.,* No. 50, Amer. Meteor. Soc., 167–221.

Dotzek, N., 2001: Tornadoes in Germany. *Atmos. Res.,* **56,** 233–251.

Evans, J. S., and R. H. Johns, 1996: Significant tornadoes in the Big Horn Mountains of Wyoming. Preprints, *18th Conf. on Severe Local Storms,* San Francisco, CA, Amer. Meteor. Soc., 636–640.

Farrell, R. J., and T. N. Carlson, 1989: Evidence for the role of the lid and underunning in an outbreak of tornadic thunderstorms. *Mon. Wea. Rev.,* **117,** 857–871.

Forbes, G. S., 1998: Topographic influences on tornadoes in Pennsylvania. Preprints, *19th Conf. on Severe Local Storms,* Minneapolis, MN, Amer. Meteor. Soc., 269–272.

Fujita, T. T., 1989: The Teton–Yellowstone tornado of 21 July 1987. *Mon. Wea. Rev.,* **117,** 1913–1940.

——, 1993: Plainfield tornado of 28 August, 1990. *The Tornado: Its Structure, Dynamics, Prediction and Hazards, Geophys. Monogr.,* No. 79, Amer. Geophys. Union, 1–17.

Giordano, L. A., and J. M. Fritsch, 1991: Strong tornadoes and flash-flood-producing rainstorms during the warm season in the mid-Atlantic region. *Wea. Forecasting,* **6,** 437–455.

Grazulis, T. P., 1993: *Significant American Tornadoes, 1680–1991.* Environmental Films, St. Johnsbury, VT, 1326 pp.

——, 1997: *Significant Tornadoes Update, 1992–1995.* Environmental Films, St. Johnsbury, VT, 117 pp.

Hannesen, R., N. Dotzek, H. Gysi, and K. D. Beheng, 1998: Case study of a tornado in the upper Rhine Valley. *Meteor. Z.,* **7,** 163–170.

——, ——, and J. Handwerker, 2000: Radar analysis of a tornado over hilly terrain on 23 July 1996. *Phys. Chem. Earth,* **25B,** 1079–1084.

Johns, R. H., and R. A. Dorr Jr., 1996: Some meteorological aspects of strong and violent tornado episodes in New England and eastern New York. *Natl. Wea. Dig.,* **20** (4), 2–12.

Johnson, R. H., and B. E. Mapes, 2001: Mesoscale processes and severe convective weather. *Severe Convective Storms, Meteor. Monogr.,* No. 50, Amer. Meteor. Soc., 71–122.

LaPenta, K. D., L. F. Bosart, T. J. Galarneau Jr., and M. J. Dickinson, 2005: A multiscale examination of the 31 May 1998 Mechanicville, New York, F3 tornado. *Wea. Forecasting,* **20,** 494–516.

Ludlam, D. M., 1970: *Early American Tornadoes, 1586–1870. Historical Monogr.,* Amer. Meteor. Soc., 219 pp.

Monteverdi, J. P., and J. Quadros, 1994: Convective and rotational parameters associated with three tornado episodes in northern and central California. *Wea. Forecasting,* **9,** 285–300.

NCDC, 1973–1995: *Storm Data*. Vols. 15–37. [Available from National Climatic Data Center, 151 Patton Ave., Asheville, NC 28801.]

Nuss, W. A., 1986: Observations of a mountain tornado. *Mon. Wea. Rev.,* **114,** 233–237.

Piaget, A., 1976: L'evolution orageuse au nord des Alpes et la tornade de Jura vaudois du 26 auot 1971 (Evolution of a storm north of the Alpes and the Jura Mts. tornado of Aug. 26, 1971). *Veröffentlichungen der MeteoSchweiz,* Vol. 35, 114 pp.

Rasmussen, E. N., 2003: Related supercell and tornado forecast parameters. *Wea. Forecasting,* **18,** 530–535.

Riley, G. T., and L. F. Bosart, 1987: The Windsor Locks, Connecticut tornado of 3 October 1979: An analysis of an intermittent severe weather event. *Mon. Wea. Rev.,* **115,** 1655–1677.

Rotunno, R., 1993: Supercell thunderstorm and modeling theory. *The Tornado: Its Structure, Dynamics, Prediction and Hazards, Geophys. Monogr.,* No. 79, Amer. Geophys. Union, 57–73.

——, J. B. Klemp, and M. L. Weisman, 1988: A theory for strong, long-lived squall lines. *J. Atmos. Sci.,* **45,** 463–485.

Seimon, A., and D. Fitzjarrald, 1994: Topographic influences on mesocyclone evolution and storm structure in an extreme supercell thunderstorm over rough terrain. Preprints, *Sixth*

Conf. on Mesoscale Processes, Portland, OR, Amer. Meteor. Soc., 513–514.

Szoke, E. J., M. L. Weisman, J. M. Brown, F. Caracena, and T. W. Schlatter, 1984: A subsynoptic analysis of the Denver tornadoes of 3 June 1981. *Mon. Wea. Rev.,* **112,** 790–808.

Thompson, R. L., R. Edwards, J. A. Hart, K. L. Elmore, and P. M. Markowski, 2003: Close proximity soundings within supercell environments obtained from the Rapid Update Cycle. *Wea. Forecasting,* **18,** 1243–1261.

Trapp, R. J., E. D. Mitchell, T. A. Tipton, D. W. Effertz, A. I. Watson, D. L. Andra, and M. A. Magsig, 1999: Descending and nondescending tornadic vortex signatures detected by WSR-88Ds. *Wea. Forecasting,* **14,** 625–639.

Wasula, A. C., L. F. Bosart, and K. D. LaPenta, 2002: The influence of terrain on the severe weather distribution across interior eastern New York and western New England. *Wea. Forecasting,* **17,** 1277–1289.

Weisman, M. L., and J. B. Klemp, 1982: The dependence of numerically simulated convective storms on vertical wind shear and buoyancy. *Mon. Wea. Rev.,* **110,** 504–520.

——, and ——, 1984: The structure and classification of numerically simulated convective storms in directionally varying wind shears. *Mon. Wea. Rev.,* **112,** 2479–2498.

——, and R. Rotunno, 2000: The use of vertical wind shear versus helicity in interpreting supercell dynamics. *J. Atmos. Sci.,* **57,** 1452–1472.

——, M. S. Gilmore, and L. J. Wicker, 1998: The impact of convective storms on their local environment: What is an appropriate ambient sounding? Preprints, *19th Conf. on Severe Local Storms,* Minneapolis, MN, Amer. Meteor. Soc., 238–241.

Wicker, L. J., 2000: The role of low-level shear, mid-level shear, and buoyancy in the intensity of modelled low-level mesocyclones. Preprints, *20th Conf. on Severe Local Storms,* Orlando, FL, Amer. Meteor. Soc., 587–590.

——, M. Kay, and M. P. Foster, 1996: Stormtipe-95: A convective storm forecast experiment using a three-dimensional cloud model. Preprints, *18th Conf. on Severe Local Storms,* San Francisco, CA, Amer. Meteor. Soc., 376–380.

Wilhelmson, R. B., and L. J. Wicker, 2001: Numerical modeling of severe local storms. *Severe Convective Storms, Meteor. Monogr.,* No. 50, Amer. Meteor. Soc., 123–166.